JOC The Journal of Organic Chemistry

Article

pubs.acs.org/joc

Arrays of Molecular Rotors with Triptycene Stoppers: Surface Inclusion in Hexagonal Tris(*o*-phenylenedioxy)cyclotriphosphazene

Jiří Kaleta,*[,†] Paul I. Dron,[‡] Ke Zhao,[⊥] Yongqiang Shen,[⊥] Ivana Císařová,[§] Charles T. Rogers,[⊥] and Josef Michl[†,‡]

[†]Institute of Organic Chemistry and Biochemistry, Academy of Sciences of the Czech Republic, Flemingovo nám. 2, 16610 Prague, Czech Republic

[‡]Department of Chemistry and Biochemistry and [⊥]Department of Physics, University of Colorado, Boulder, Colorado 80309, United States

[§]Department of Inorganic Chemistry, Faculty of Science, Charles University in Prague, Hlavova 2030, 12840 Prague, Czech Republic

Supporting Information

ABSTRACT: A new generation of rod-shaped dipolar molecular rotors designed for controlled insertion into channel arrays in the surface of hexagonal tris(*o*-phenylenedioxy)cyclotriphosphazene (TPP) has been designed and synthesized. Triptycene is used as a stopper intended to prevent complete insertion, forcing the formation of a surface inclusion. Two widely separated ^{13}C NMR markers are present in the shaft for monitoring the degree of insertion. The structure of the two-dimensional rotor arrays contained in these surface inclusions was examined by solid-state NMR and X-ray powder diffraction. The NMR markers and the triptycene stopper functioned as designed, but half of the guest molecules were not inserted as deeply into the TPP channels as the other half. As a result, the dipolar rotators were distributed equally in two planes parallel to the crystal surface instead of being located in a single plane as would be required for ferroelectricity. Dielectric spectroscopy revealed rotational barriers of ~4 kcal/mol but no ferroelectric behavior.

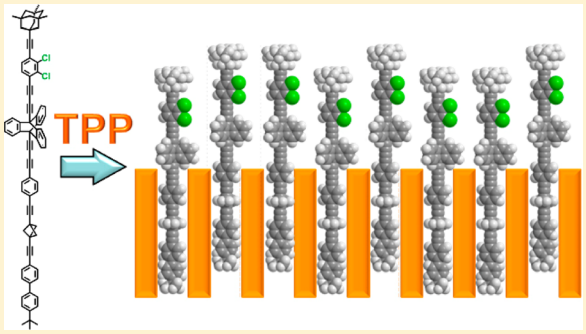

INTRODUCTION

Artificial molecular rotors have attracted the unflagging attention of scientists over the last few decades, as documented by numerous articles, reviews, and book chapters.[1−18] We are interested in the design, preparation, and characterization of two-dimensional rotor arrays with a well-defined ground state. The most interesting of these would be ferroelectric with the dipoles of all of the rotators aligned. This might be achievable at a low temperature in a planar triangular lattice of strongly coupled rotors with a very low rotational barrier.[19]

Our approach has been to find a host crystal with a suitable facet that contains trigonally arranged channels into which the axles of the rotors can be tightly included as guests.[10,15] For the host, we chose the hexagonal form of tris-*o*-(phenylenedioxy)-cyclotriphosphazene, commonly abbreviated as TPP (Figure 1). It is a molecular crystal with a layered structure containing parallel channels with a 4.5−5.0 Å internal diameter oriented perpendicular to the layers and located in a triangular lattice ~11.5 Å apart.[20] TPP is chemically quite inert and is transparent down to 300 nm. It can be readily prepared from commercially available chemicals, its ^{13}C and ^{31}P NMR spectra are simple, and the ring currents of its benzene rings modify the chemical shifts of the guest nuclei by several ppm, allowing the extent of guest inclusion to be readily recognized by solid state NMR if the guest contains suitable NMR markers. Its disadvantages are sensitivity to oxygen during long-term storage in air and the existence of a competing monoclinic form whose formation needs to be avoided.

The formation of a two-dimensional array of rotors requires the production of a surface inclusion in which the guests are present only at the surface and are unable to penetrate inside the crystal. Little is known about the design of artificial surface inclusions, but it seems reasonable that the inclusion of a fat "stopper" in the rod to be inserted would lead to the desired structure. Because TPP is a molecular crystal, it is able to expand its lattice relatively easily when guests are included, increasing the channel diameter and interchannel distance by up to ~10%.[15] This offers a valuable independent method for recognizing inclusion by X-ray powder diffraction (XRD), but also causes a fair degree of uncertainty in estimates of the maximum size of an acceptable guest and the necessary minimum size of a stopper. Admittedly, size is not the only factor that controls the formation of inclusion compounds, and the relative lattice energies of the inclusion compound and of the separate crystals of pure host and guest are critical. After

Received: March 24, 2015
Published: May 6, 2015

DOI: 10.1021/acs.joc.5b00661
J. Org. Chem. 2015, 80, 6173−6192

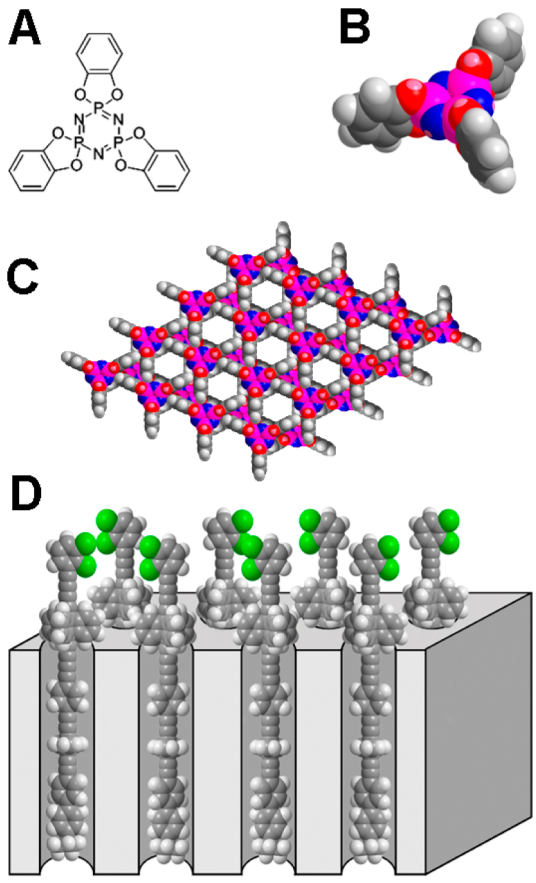

Figure 1. Structure of hexagonal TPP. (A) Chemical structure and (B) space-filling model of a single TPP molecule. (C) Two successive layers of the crystal viewed from above. (D) Idealized model of rotor insertion.

some initial searching,[10,11,14,15,21] we are now able to report a host–guest combination that promises to reliably lead to surface inclusions.

As shown in Figure 1 (cf. Chart 1), rotor guests are designed to form surface inclusions by inserting a long shaft (a) but being unable to insert a bulky stopper (b) that separates the shaft from an axle (c) that carries a dipolar rotator (d). In an attempt to discourage undesirable aggregation of neighboring axles and the associated rotators, structure **2** is terminated with a bulky group (e).

Long Shaft (a). This part of molecules **1** and **2** is similar to some of the rotor shafts that were used in our previous work with TPP inclusions and showed high affinity for the channels.[21,22] A recent novelty is the presence of two bulky saturated groups, *tert*-butyl at one end and bicyclo[1.1.1]penta-1,3-diyl, near the center of the segment that is to be included. These groups are meant to serve three purposes: (i) they facilitate synthetic manipulations by increasing solubility, (ii) their bulk helps to fix the shaft firmly against the channel walls, limiting its possible wobbling motion,[22] and (iii) because their ^{13}C NMR shifts are situated in spectral regions that avoid overlap with signals of other rotor carbons and TPP, they reveal the inclusion of the shaft in the channel.

Triptycene Stopper (b). Our initial attempts to form a regular array of dipolar rotors on the surface of TPP were plagued by uncertainties related to the choice of a reliable stopper, because even the *p*-carborane stopper, whose van der Waals diameter greatly exceeds the internal diameter of an

Chart 1. Structures 1–3: Long Shaft (a), Triptycene Stopper (b), Axle (c), Dipolar Rotator (d), and Bulky Terminus (e)

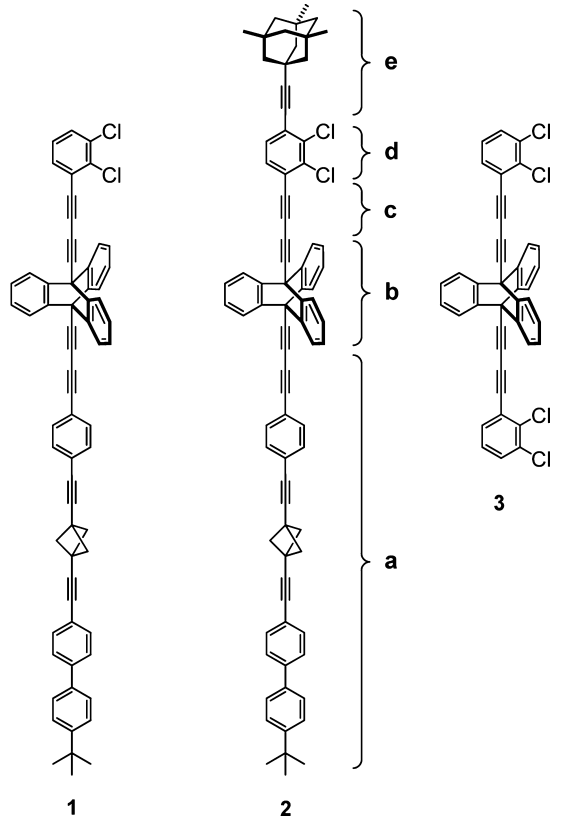

empty TPP channel, is sometimes able to enter.[10,15] Presently, we examine the use of triptycene derivatives and establish that the equatorial diameter of triptycene is sufficient to prevent this undesirable behavior. Triptycenes are easily accessible from cheap and commercially available precursors, have high chemical stability, and are easily provided with substituents at the bridgehead carbons.[23–26]

Axle (c). The use of butadiynylene instead of ethynylene as an axle extends the distance between the rotator and the triptycene stopper, thus minimizing the rotational barrier, and it is synthetically convenient. However, it also increases the flexibility of the axle, whose bending might permit an undesirable aggregation of neighboring dipoles.

Dipolar Rotator (d). The choice of rotators was driven by the desire to have not only a small barrier to rotation and a sizable dipole moment, but also a diameter that will be large enough to discourage entry into the TPP channel, because otherwise the molecular rotor could prefer to insert its rotator instead of its shaft. As before, we used 2,3-dichlorophenyl, whose ~7.8 Å diameter[27] significantly exceeds the nominal 4.5–5.0 Å internal diameter of the channel. The dipole moment of *o*-dichlorobenzene is 2.51 D.[28]

Bulky Terminus (e). The intended function of this third modification in rotor design is to constrain possible contacts between neighboring 2,3-dichloro-1,4-phenylene rotators permitted by the flexibility of the butadiyne axle. It also prevents a "backward" insertion of the rotor into a TPP channel. This building block thus had to fulfill three major criteria: (i) its diameter had to be larger than that of the rotator, both to keep the rotators apart and to prevent channel entry, (ii) it had to avoid mechanical contact with the rotator in order to keep the

DOI: 10.1021/acs.joc.5b00661
J. Org. Chem. 2015, 80, 6173–6192

Scheme 1. Preparation of the Shaft (10)

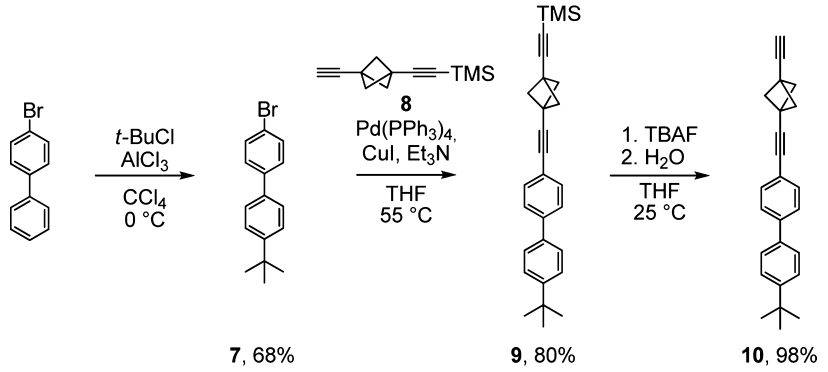

rotational barrier small, and (iii) it had to be nonpolar and preferably trigonally symmetrical. We chose the 3,6,9-trimethyladamantyl unit.

The guest molecules that were used in this study are listed in Chart 1. Symmetric structure **3**, with two 2,3-dichlorophenyl rotators, was not expected to form an inclusion compound and was prepared to check the inability of a 2,3-dichlorophenyl moiety to enter an empty TPP channel that was not stretched by another large included guest (this group is known to enter when attached to *p*-carborane[21]).

RESULTS

We describe the synthesis of **1**–**3**, assignment of ^{1}H and ^{13}C peaks in their solution NMR spectra, single-crystal X-ray structures of four related compounds, the formation of inclusion compounds with TPP, and the characterization of these inclusions by solid-state NMR spectroscopy, X-ray powder diffraction, and temperature-dependent dielectric behavior.

Synthesis. The synthetic approach to **1** and **2** respected the expected negligible solubility of the final products. The approach is based on the preparation of two adequately soluble molecular fragments (the bicyclo[1.1.1]pentane-based shaft **4** and a triptycene derivative with a 2,3-dichlorophenyl or a 2,3-dichloro-1,4-phenylene rotator **5** or **6**) whose Sonogashira coupling produces the poorly soluble final products.

Synthesis of Rotors 1–3. Synthesis of the long shaft (a) of molecules **1** and **2** (Chart 1) started with Friedel–Crafts alkylation of 4-bromobiphenyl to **7**,[29] whose Sonogashira coupling with ((3-ethynylbicyclo[1.1.1]pent-1-yl)ethynyl)-trimethylsilane[30,31] (**8**) afforded silyl derivative **9** (Scheme 1). The trimethylsilyl group was removed using TBAF, and corresponding alkyne **10** was obtained in a nearly quantitative yield.

The triptycene stopper (b, Chart 1) was made in eight steps from commercially available 9,10-dibromoanthracene (**11**). The known route from **11** to 9,10-diethynyltriptycene (**12**) was slightly modified and scaled up, allowing the preparation of multigram quantities of **12**. Anthracene **11** was coupled with TMSA in refluxing Et_2NH under $PdCl_2(PPh_3)_2$/CuI catalysis to obtain the silylated derivative **13** in excellent yield.[32] Diels–Alder addition of benzyne, generated in situ from anthranilic acid and isoamyl nitrite, to anthracene **13** afforded the desired silylated triptycene **14**.[33] Both trimethylsilyl groups were removed in an almost quantitative yield using either K_2CO_3 in the mixture of THF and methanol[33] or TBAF in THF.

Double lithiation of **12** followed by the reaction with paraformaldehyde gave diol **15**, whose oxidation using Dess–Martin periodinane in CH_2Cl_2 at room temperature yielded dialdehyde **16**. Poor solubility of diol **15** in CH_2Cl_2, even at room temperature, did not allow such transformation using the standard protocol for Swern oxidation. The reaction of **16** with CBr_4 in the presence of PPh_3 afforded tetrabromo derivative **17**, whose dehydrobromination with *n*-BuLi was followed by capturing the dilithiated species with TMSCl. The desired disilylated tetrayne **18** was isolated in high yield. Desymmetrization of **18** using MeLi in THF at 10 °C gave a statistical mixture of **19** and **20** in isolated yields of 48% and 39%, respectively (Scheme 2).

The next focus was synthesis of the bulky 3,5,7-trimethyladamantyl unit required for rotor **2** (Scheme 3). The $AlBr_3$-catalyzed Friedel–Crafts reaction of commercially available 1-bromo-3,5,7-trimethyladamantane (**21**) in liquid vinyl bromide introduced the 2,2-dibromoethyl moiety and

Scheme 2. Synthesis of 19 and 20

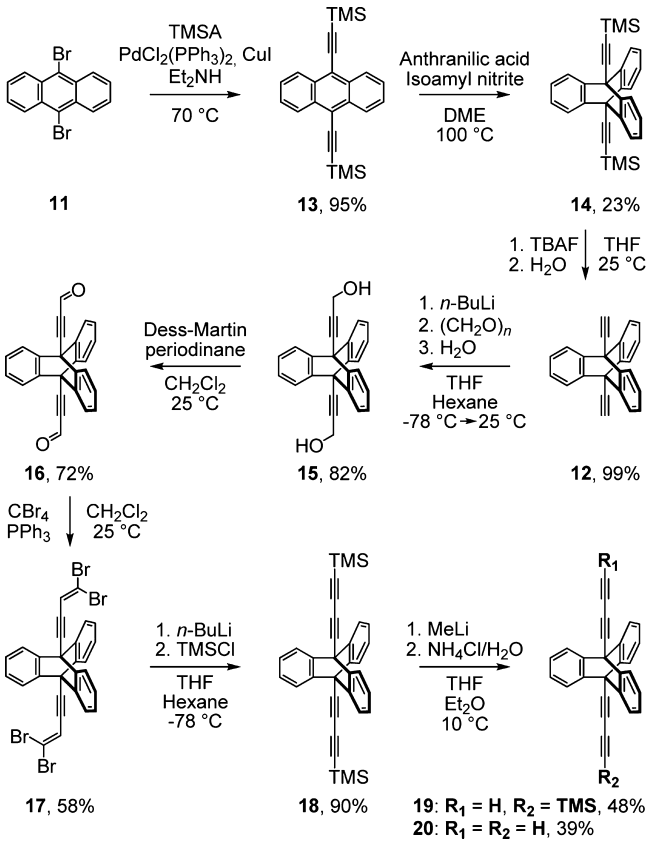

DOI: 10.1021/acs.joc.5b00661
J. Org. Chem. 2015, 80, 6173–6192

Scheme 3. Construction of Rotator 25

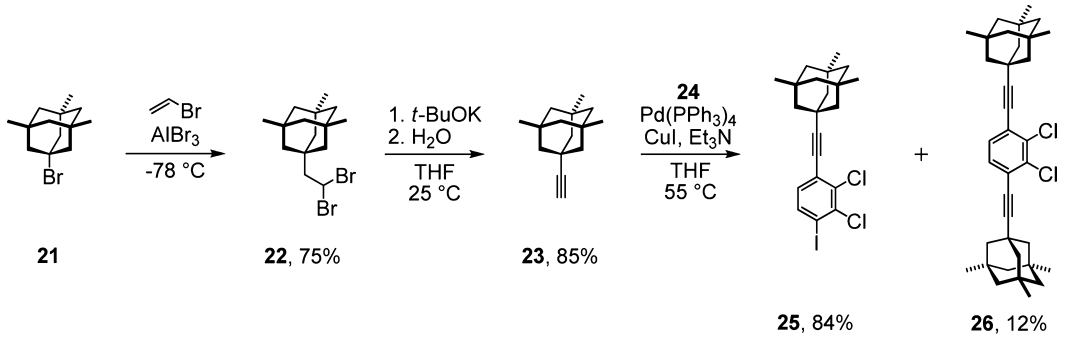

yielded **22**. A modification of the published procedure[34] allowed us to increase the isolated yield from the original 40% to 75%. Alkyne **23** was obtained by treatment with *t*-BuOK.[34] A rapid trans dehydrobromination in the first step was followed by a geometrically disfavored cis elimination and a 3 day reaction time was required. Sonogashira coupling with excess 1,4-diiodo-2,3-dichlorobenzene (**24**)[35] at a slightly elevated reaction temperature (40 °C, most likely required due to the high steric demand of the adamantyl unit) gave a mixture containing **25** as the expected major product and **26** as a minor side product (Scheme 3).

Rotators **27** and **25** were connected with triptycene stopper **19** using Sonogashira coupling. Terminal alkynes **5** and **6** were then liberated from their TMS derivatives **28** and **29**, respectively, in almost quantitative yields using TBAF (Scheme 4).

Scheme 4. Preparation of Alkynes 5 and 6

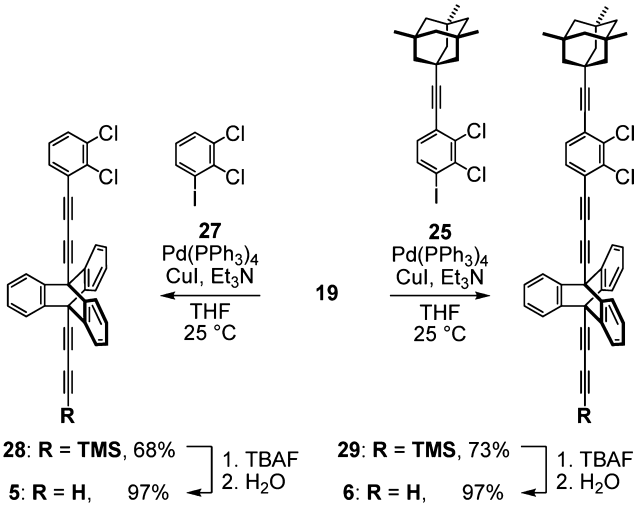

The last step in the synthesis of the long shaft (**4**) was the coupling of alkyne **10** with excess 1,4-diiodobenzene, which proceeded in 78% yield. The Sonogashira coupling of iodo derivative **4** with alkynes **5** and **6** afforded the desired molecular rotors **1** and **2** in 76 and 70% yield, respectively (Scheme 5). The low solubility of the final products simplified their purification, because both compounds precipitated from the reaction mixture and were easily isolated using a centrifuge and filtration.

Symmetric rotor **3** was made from tetrayne **20** and 1,2-dichloro-3-iodobenzene (**27**) using standard conditions for

Scheme 5. Final Assembly of Molecular Rotors 1 and 2

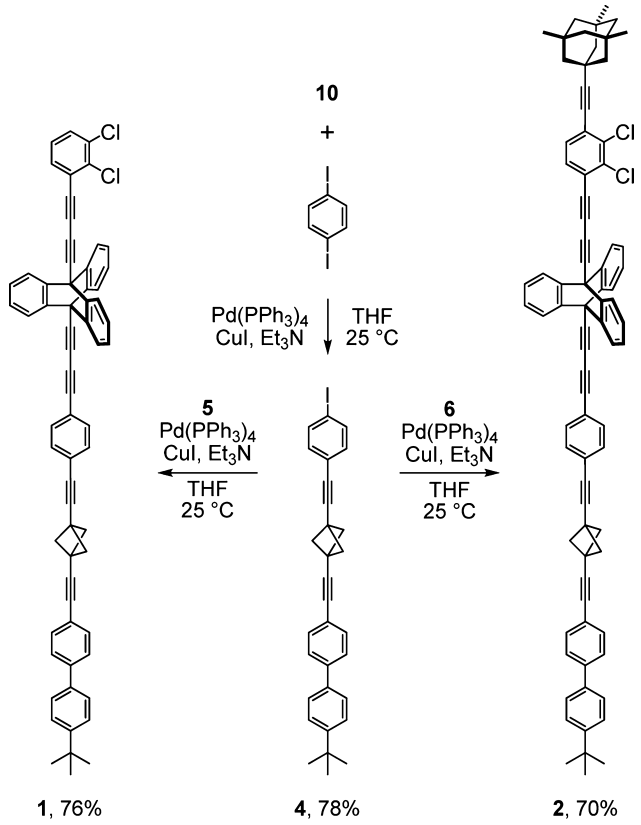

Sonogashira coupling. A double reaction on both terminal alkynes of **20** resulted in 78% yield of **3**.

Unsuccessful Attempts to Prepare Related Rotors. The benzene ring connecting alkyne **10** with the triptycene stopper in **5** and **6** is not crucial for the rotor function, and two attempts were made to reduce the length of the shaft (a, Chart 1) with the expectation that the shorter molecules would be more soluble. Unfortunately, both attempts failed.

In the first approach, simple monosilylated triptycene **30**, obtained by statistical desymmetrization of **14** in an acceptable isolated yield of 57% (Scheme 6), was used to mimic the behavior of the less easily accessible alkyne **5** or **6**. Cadiot–Chodkiewicz coupling between alkyne **10** and alkynyl bromide **31**, which was made by $AgNO_3$-catalyzed NBS bromination of **30** (Scheme 6), did not lead to the expected product, and the ^1H NMR spectrum of the crude reaction mixture contained mostly the product of oxidative homocoupling of alkyne **10**.

DOI: 10.1021/acs.joc.5b00661
J. Org. Chem. 2015, 80, 6173–6192

Scheme 6. Statistical Desymmetrization of 14 and Bromination of 30

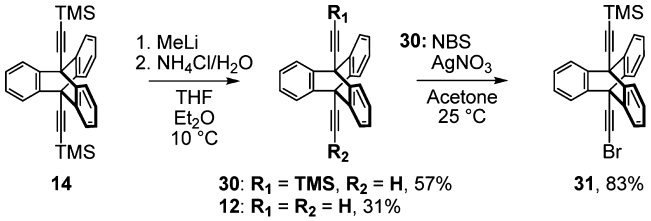

The second approach was inspired by the preparation of conjugated polyynes, where the crucial step is a stepwise synthesis of an internal triple bond based on the Fritsch–Buttenberg–Wiechell rearrangement.[36,37] At first, alkyne **10** was converted to ynone **32** in two steps (Scheme 7, route A). Lithiation of **10** followed by a reaction with paraformaldehyde resulted in alcohol **33**, which was subsequently oxidized to ynone **32** by Swern oxidation.

Scheme 7. Possible Routes to Ynone 32

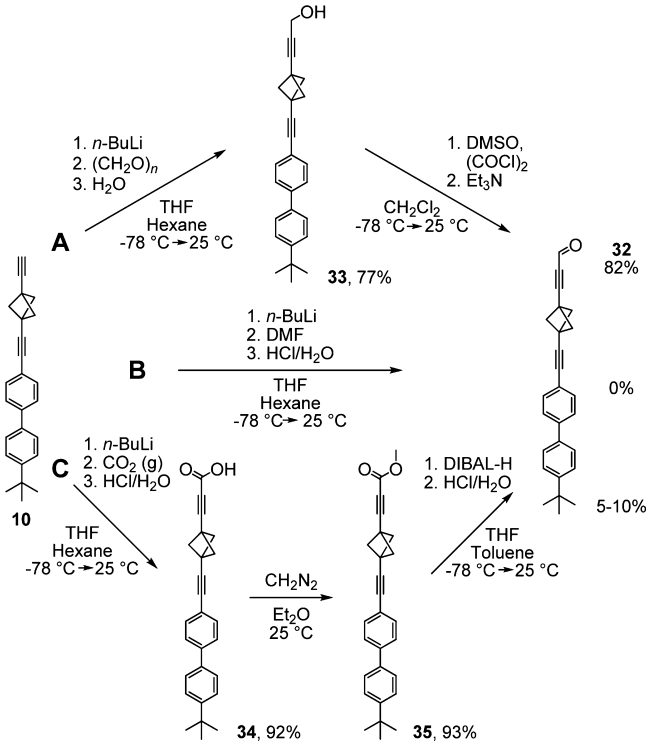

A one-step conversion of **10** to **32** based on the formylation of the lithiated alkyne with anhydrous DMF did not produce any of the expected **32**, and only starting material **10** was isolated from the crude reaction mixture (Scheme 7, route B). In contrast, carboxylation of the lithium acetylide derived from **10** by gaseous CO_2 gave acid **34** in excellent yield. Subsequent esterification by ethereal diazomethane also afforded methyl ester **35** in an almost quantitative yield. The following DIBAL reduction failed, however, and ^{1}H NMR of the crude reaction mixture contained starting material **35** and mere traces of the desired ynone **32** (Scheme 7, route C).

The addition of lithiated **30** to ynone **32** resulted in a nearly quantitative yield of racemic alcohol **36**, whose Swern oxidation gave ketone **37** in 79% yield (Scheme 8). However, the reaction with CBr_4 in the presence of PPh_3 provided desired product **38** in a synthetically useless yield of less than 5% (based on ^{1}H NMR). The failure of the first approach and the poor yield of dibromo derivative **38** during this second approach prompted us not to pursue additional attempts to reduce the length of the shaft (a).

The van der Waals diameter of the 3,5,7-trimethyladamantyl group (~6.9 Å) should discourage aggregation of neighboring rotators after the insertion of **2** into TPP but is unlikely to prevent bending of the butadiyne axle (c). Accordingly, the sterically more demanding tris(trimethylsilyl)silyl unit, whose van der Waals diameter is ~8.0 Å, was chosen as a second possible candidate. The intended synthesis followed the reactions shown in Schemes 4 and 5 with an $Si(TMS)_3$ group in place of the 3,5,7-trimethyladamantyl unit. Because little is known about the chemical stability of $Si(TMS)_3$ in the presence of other silyl protecting groups, we synthesized silane **39** containing both TMS and $Si(TMS)_3$ to test for selective TMS removal.

Alkyne **40** was easily available from $ClSi(TMS)_3$ and BrMgCCH in THF at room temperature.[38] Its Sonogashira coupling with bromo derivative **41** gave desired model structure **39** in 82% yield. An attempted removal of TMS using K_2CO_3 in THF/MeOH failed. Mild conditions that allow selective cleavage of TMS in the presence of TES even at room temperature[39,40] caused quantitative removal of the $Si(TMS)_3$ group even though the reaction was run at 0 °C. A reaction of **39** with MeLi in THF clearly demonstrated that the $Si(TMS)_3$ group is much more labile than TMS, because the same reaction conditions had been used twice in this work to remove the TMS group at 5–10 °C (Schemes 2 and 6). $Si(TMS)_3$ was cleaved preferentially at −78 °C, and compounds **42** and **43** were isolated in almost quantitative yields (Scheme 9). A combination of the sterically protected triple bond of alkyne **40** with the more sterically demanding tetrahalo derivative **24** prevented the Sonogashira coupling reaction entirely. The desired product was not formed even at 80 °C, and only the starting materials were isolated from the crude reaction mixture (Scheme 9).

The observation that alkyne **40** does not undergo Sonogashira coupling with sterically demanding substrate **24**, whereas $ClSi(TMS)_3$ reacts with deprotonated alkynes, prompted an alternative strategy for reaching the desired rotator. One iodine atom in **24** was substituted by a triple bond, and the resulting acetylide was coupled with $ClSi(TMS)_3$. Tetrahalo derivative **24** was desymmetrized using Sonogashira coupling with TMSA. The reaction yielded alkynes **44** and **45** in 69 and 25% yield, respectively, at an elevated temperature (40 °C). Deprotection of **44** using TBAF in THF gave the unstable terminal alkyne **46** in 90% yield as a white crystalline solid that turned black instantly after exposure to air. Compound **46** was therefore immediately lithiated using LiHMDS and treated with $ClSi(TMS)_3$. The triple bond was indeed silylated, but iodine was surprisingly replaced by hydrogen at the same time; dichloro derivative **47** was isolated as the only product in 76% yield (Scheme 10).

The unpredictable reactivity of $Si(TMS)_3$-substituted derivatives prompted us to give up additional attempts to use the $Si(TMS)_3$ unit as the bulky group (e, Chart 1).

Molecular Rotors. *Solution ^{1}H and ^{13}C NMR.* Except for the signals of several triple bond carbons, all ^{1}H NMR and most of the ^{13}C NMR signals of **1**–**3** were assigned using ^{1}H–^{1}H COSY, ^{13}C attached-proton test (APT), HSQC, and HMBC (Figure 2 and Supporting Information).

DOI: 10.1021/acs.joc.5b00661
J. Org. Chem. 2015, 80, 6173–6192

Scheme 8. Attempted Synthesis of Dibromide 38

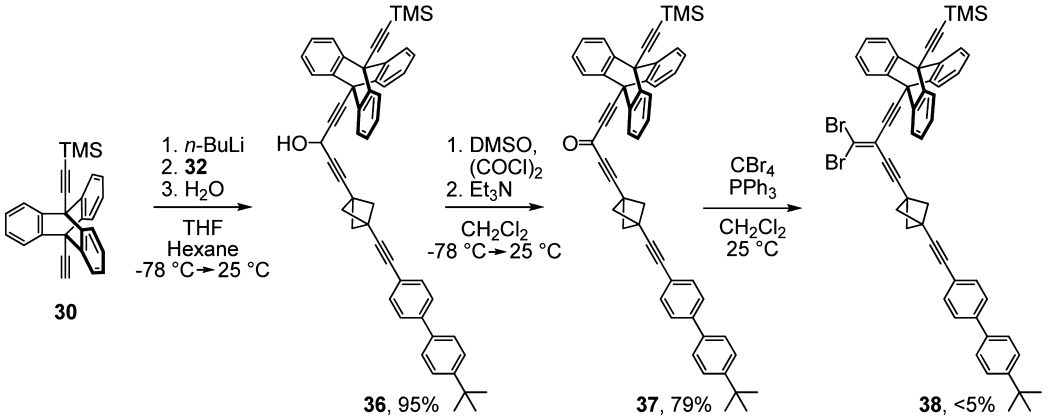

Scheme 9. Attempted TMS Removal and Coupling with 24

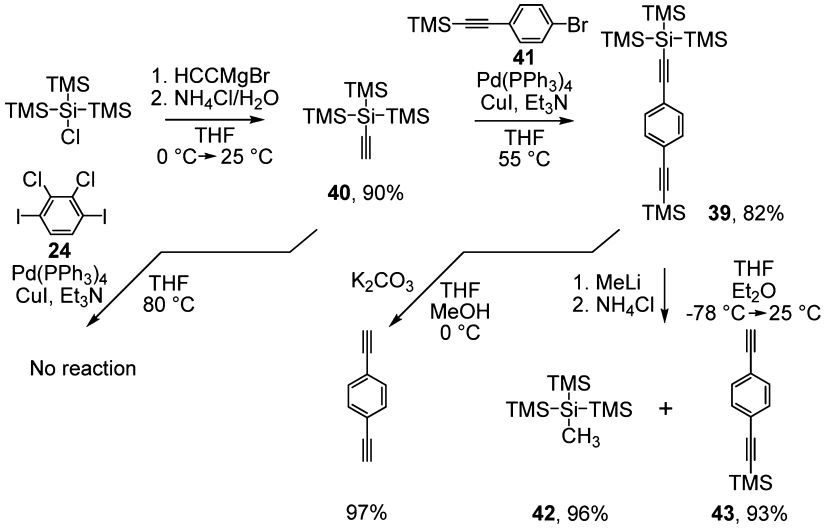

Scheme 10. Desymmetrization of 24 and Silylation of 46

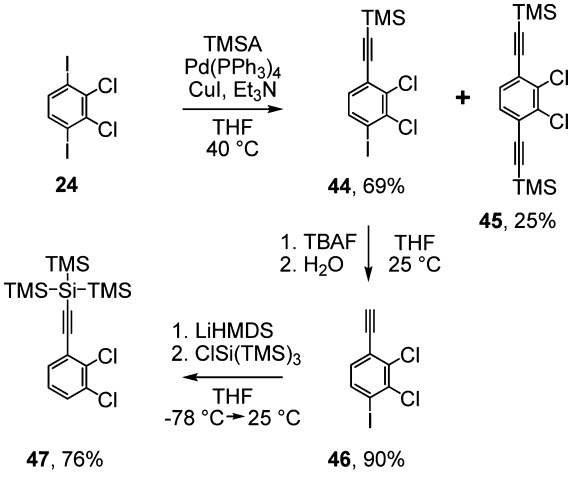

Crystal Packing. Intermolecular interactions between rotor molecules codetermine the structures of surface inclusions, and it would be helpful to understand how the rotors prefer to pack in a crystal lattice. Attempts to obtain high-quality crystals of **1**–**3** were unsuccessful, but we were able to grow suitable single crystals of **16**, **17**, **20**, and **26** by slow evaporation of CH_2Cl_2 solutions and examine their crystal packing by X-ray analysis. Compound **16** crystallized in the triclinic crystal system and P-1 space group, and **17** and **26** crystallized in the monoclinic crystal system and $C2/c$ and $P2_1/c$ space groups, respectively. Tetrayne **20** formed orthorhombic crystals with a *Pbca* space group. ORTEP representations of single molecules of **16**, **17**, and **20**, along with space-filling models showing two neighboring molecules and their arrangement in one crystal layer, are shown in Figure 3. They all crystallize in the same manner with two paddles of a triptycene core embracing an ethynyl unit of a neighbor.

Inclusion Compounds. These were prepared by milling and subsequent extended annealing at 70 °C, sometimes followed by brief annealing at 235 °C. The samples will be referred to by symbols such as X%**1**@TPP-d_{12}(70) or X%**1**@TPP-d_{12}(235), respectively, where X equals 5 or 16, and stands for the molar % of guest **1**. These concentrations were chosen based on analogy with similar previously published inclusion complexes.[14,21]

Solid-State ^{13}C and ^{31}P NMR. The NMR behavior of the inclusion compounds was studied by ^{13}C cross-polarization magic-angle spinning (CP MAS), ^{31}P CP MAS, and ^{31}P single pulse excitation (SPE).

Rotor 1. The solid-state ^{13}C CP MAS NMR spectrum of 5%**1**@TPP-d_{12}(70) shows a similar peak pattern as the ^{13}C solution NMR with peaks shifted upfield or downfield. It also

DOI: 10.1021/acs.joc.5b00661
J. Org. Chem. 2015, 80, 6173–6192

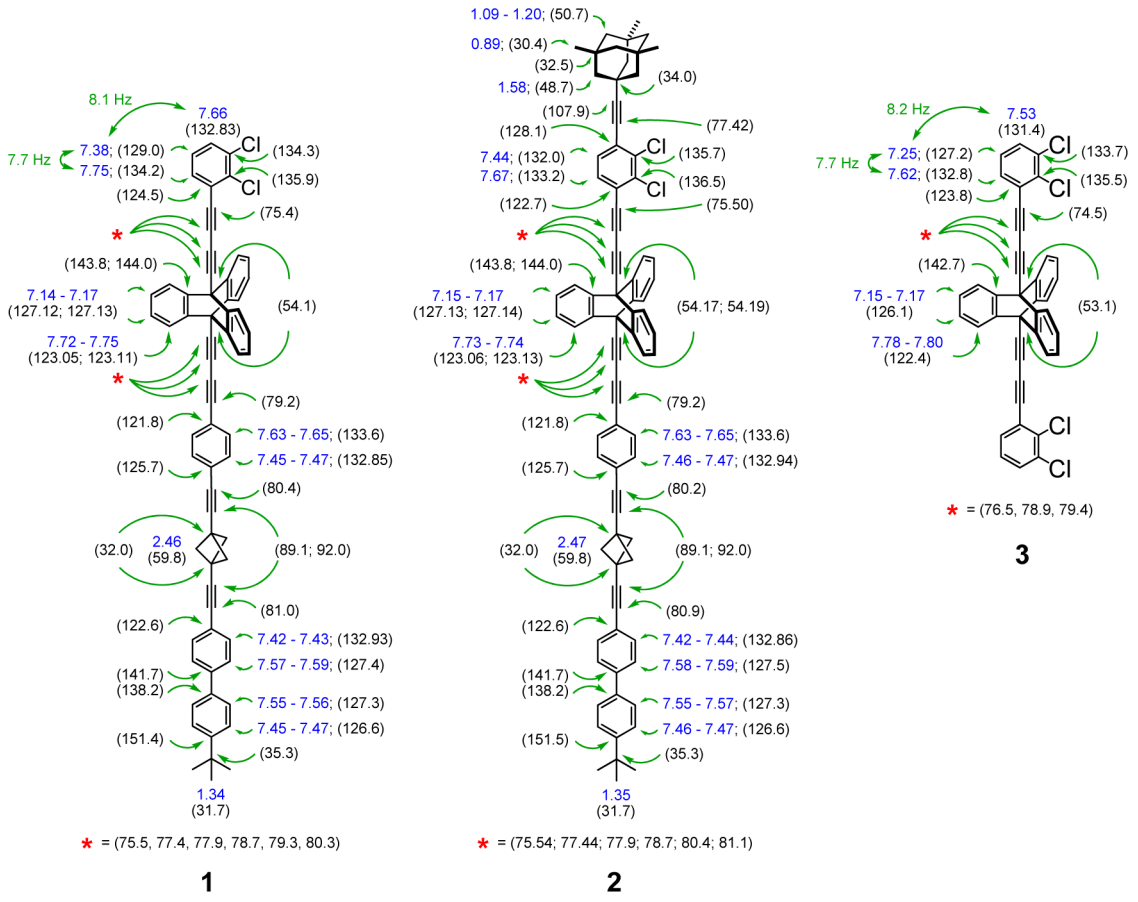

Figure 2. ^{1}H (blue) and ^{13}C NMR (black) assignments in **1**, **2**, and **3**; the spectra can be found in the Supporting Information.

contains three additional peaks in the aromatic region that are due to TPP (Figure 4). In light of the complex structure of **1**, it is understandable that only some of the chemical shifts identified in the solid-state ^{13}C CP MAS NMR spectrum have been assigned.

The bicyclo[1.1.1]pentane cage present in the shaft has two characteristic signals in the ^{13}C solution NMR spectrum of rotor **1** at 32.0 (bridgehead carbons) and 59.8 ppm (bridge carbons). In the solid-state ^{13}C CP MAS NMR spectrum, the former peak is not obvious and probably overlaps with the *tert*-butyl signal at 30.4 ppm. The signal of the bridge carbons is doubled and appears as two peaks of comparable intensity, at 57.3 and 60.8 ppm.

The terminal *tert*-butyl moiety of rotor **1** has two signals in the ^{13}C solution NMR, at 31.7 ppm for the methyl carbons and at 35.3 ppm for the quaternary carbon. Two peaks of nearly equal intensities also appear in the solid-state ^{13}C CP MAS NMR spectrum of 5%**1**@TPP-d_{12}(70) but are shifted upfield to 30.4 and 32.3 ppm. It is possible that the signal of the methyl carbons is doubled similar to the signal of the bridge carbons discussed above, but it is also possible that one of the peaks belongs to the methyl carbons and the other to the quaternary carbon.

The aromatic carbon atom connected to the *tert*-butyl moiety, which appears at 151.4 ppm in the ^{13}C solution NMR, is absent in the solid-state ^{13}C CP MAS NMR of the inclusion and probably overlaps with the strong TPP signal at 144.7 ppm.

The quaternary carbon atoms in the triptycene moiety are equivalent in the ^{13}C solution NMR and have a resonance at 54.1 ppm. In the solid-state ^{13}C CP MAS NMR spectrum of the inclusion, these atoms are observed at 53.7. The acetylenic carbon atoms are characterized by several resonances between 75 and 92 ppm in the ^{13}C solution NMR. In the solid-state ^{13}C CP MAS NMR spectrum of 5%**1**@TPP-d_{12}(70), only one broad peak centered at 78.0 ppm is observed.

The ^{31}P CP MAS and ^{31}P SPE NMR spectra of the inclusions show peaks characteristic for hexagonal TPP. However, in the ^{31}P SPE NMR, additional peaks characteristic of the monoclinic form of TPP can be observed.

In an effort to convert all TPP to its hexagonal form, 5%**1**@TPP-d_{12}(70) was heated to 235 °C for 2 min. This temperature lies above the 225 °C transition point at which the guest-free hexagonal form of TPP becomes more stable than its monoclinic form[41] but is still safely below the 245 °C melting point of TPP. NMR spectra of the resulting 5%**1**@TPP-d_{12}(235) are shown in Figure S1 (Supporting Information). The ^{31}P SPE and ^{31}P CP MAS NMR spectra show that TPP is present only in its hexagonal form, but that partial decomposition of TPP to other phosphorus-containing species has occurred.

In the 20−90 ppm region of the spectrum, which contains the characteristic peaks of the triptycene and bicyclo[1.1.1]-pentane units, the ^{13}C CP MAS NMR spectra of 5%**1**@TPP-d_{12}(70) and 5%**1**@TPP-d_{12}(235) are identical, and we conclude that rotor **1** survived the heating intact. Between 110 and 150 ppm, additional peaks are observed in the ^{13}C CP MAS NMR spectrum of 5%**1**@TPP-d_{12}(235) and are attributed to decomposition products of TPP.

Rotor 2. Molecule **2** shares some structural characteristics with rotor **1** but is even more complex. Its NMR character-

DOI: 10.1021/acs.joc.5b00661
J. Org. Chem. 2015, 80, 6173−6192

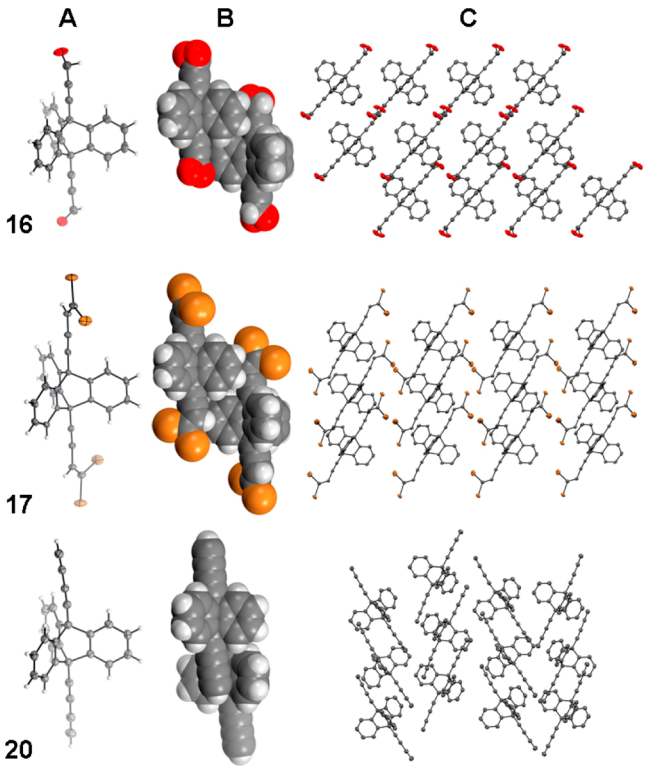

Figure 3. X-ray single crystal structure of **16**, **17**, and **20**: ORTEP representation of a single molecule (A), space-filling model of two neighboring molecules (B), and molecular packing in a crystal (C, hydrogen atoms omitted for clarity). ORTEPs drawn at the 30% level. For more detail, see the Supporting Information.

ization relies on the identification of the same moieties that were used in the description of rotor **1**.

The solid-state ^{13}C CP MAS NMR spectrum of neat rotor **2** shows a pattern similar to the ^{13}C solution NMR spectrum with some small variations in the chemical shifts. The solid-state ^{13}C CP MAS NMR spectrum of 5%**2**@TPP-d_{12}(70) is dominated by the three peaks characteristic of TPP (Figure S2, Supporting Information). The methyl carbon atoms of the *tert*-butyl moiety of the rotor appear at 32.5 ppm in solution ^{13}C NMR, in the solid state of the neat rotor, and in the ^{13}C CP MAS NMR of the inclusion compound. The only difference is that, in the spectrum of the inclusion compound, the peak is much broader, probably because it also contains the signals of the methyl carbon atoms of the adamantyl moiety. The quaternary carbon atom of the *tert*-butyl group is at almost the same position in the solution NMR (35.2 ppm) as in the neat rotor (35.5 ppm) NMR spectra, but it is not observed in the spectrum of the inclusion compound, most likely due to overlap with adamantane carbons. Similarly, the aromatic carbon attached to the *tert*-butyl moiety appears at 151.5 ppm in the solution NMR and at 150.9 ppm in the spectrum of the neat solid, but it is not observed in the spectrum of the inclusion.

The bridge carbon atoms characteristic of the bicyclo[1.1.1]-pentane cage of **2** have a resonance at 59.8 ppm in solution NMR. These carbon atoms appear at 59.9 ppm in the spectrum of the neat rotor, but the peak is broader. In the ^{13}C CP MAS NMR of the inclusion, this peak appears as a broad doublet located at the same chemical shift. The quaternary carbon atoms present in the triptycene unit have resonances at 54.17 and 54.19 ppm in solution. These atoms appear at 53.3 ppm in both the spectrum of the neat rotor and the spectrum of the

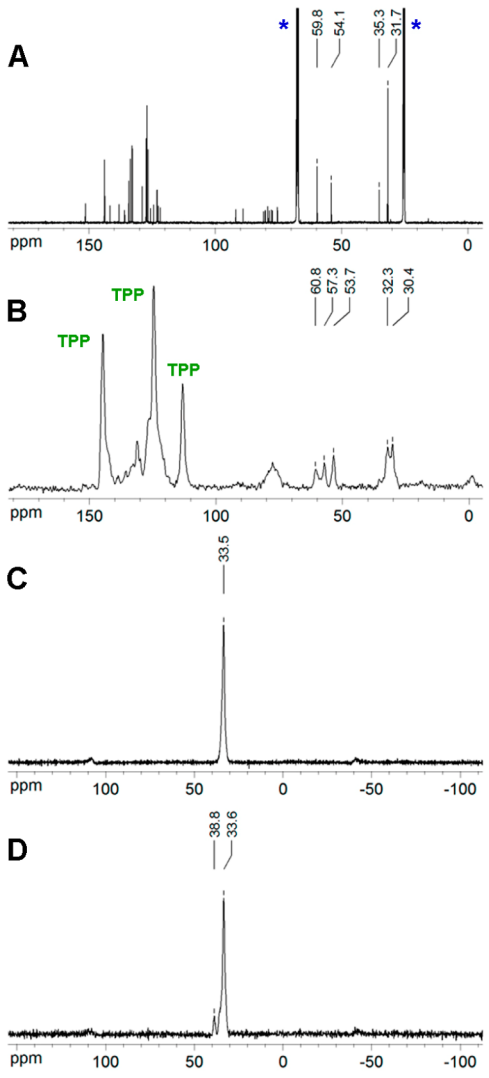

Figure 4. NMR spectra of **1** ^{13}C in THF-d_8 (*) solution (A) and of 5%**1**@TPP-d_{12}(70) ^{13}C CP MAS (B), ^{31}P CP MAS (C), and ^{31}P SPE (D).

inclusion. The acetylenic carbon atoms have chemical shifts between 76 and 93 ppm in the solution ^{13}C NMR spectrum. In the spectra of the neat rotor and of the inclusion, they appear in the same range, but the peaks are broad and poorly defined.

In the ^{31}P CP MAS spectrum of 5%**2**@TPP-d_{12}(70), the main peak lies at 33.6 ppm, indicating inclusion in the TPP channel, but an additional small peak at −1.8 ppm suggests that some TPP has decomposed. From the ^{31}P SPE NMR spectrum of the inclusion, it is obvious that ∼45% of the TPP decayed to the monoclinic form.

The ^{13}C CP MAS NMR spectrum of 16%**2**@TPP-d_{12}(70) (Figure 5) is identical to that of 5%**2**@TPP-d_{12}(70). Its ^{31}P SPE NMR spectrum reveals that the 16% loading allows all of the TPP to stay in its hexagonal form (Figure 4E). The ^{31}P CP MAS NMR spectrum contains two peaks in a 14:1 integrated intensity ratio. The stronger peak at 33.3 ppm is observed when a rotor is included in TPP, but the presence of a weak peak at −83.4 ppm suggests the presence of decomposition products.

Rotor ***3***. The solid-state ^{13}C CP MAS NMR spectrum of 5%**3**@TPP-d_{12}(70) shows a pattern almost identical to that of neat solid rotor **3**. Only three very weak additional peaks characteristic of TPP are observed (Figure 6). Besides the very

DOI: 10.1021/acs.joc.5b00661
J. Org. Chem. 2015, 80, 6173−6192

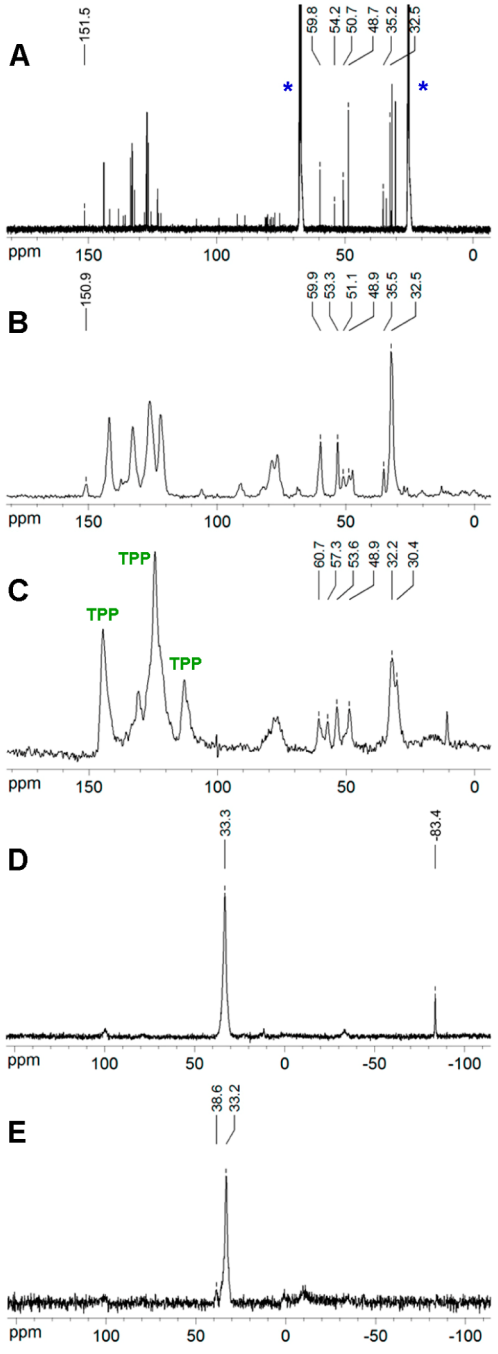

Figure 5. NMR spectra of **2** ^{13}C in THF-d_8 (*) solution (A), of neat **2** ^{13}C CP MAS (B), and of 16%**2**@TPP-d_{12}(70) ^{13}C CP MAS (C), ^{31}P CP MAS (D), and ^{31}P SPE (E).

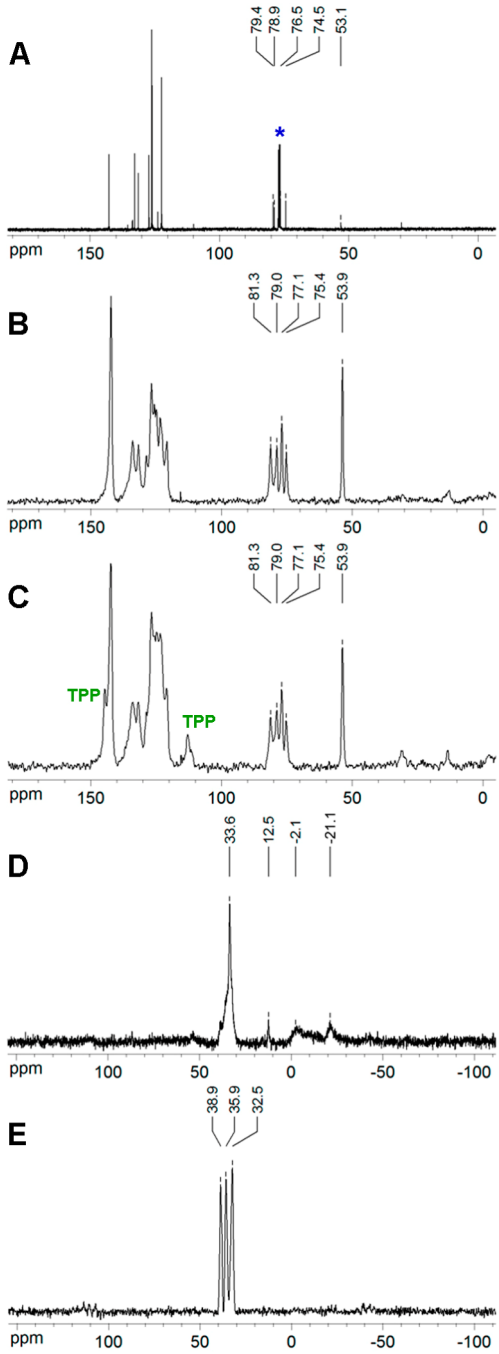

Figure 6. NMR spectra of **3** ^{13}C in $CDCl_3$ (*) solution (A), of neat **3** ^{13}C CP MAS (B), and of attempted 5%**2**@TPP-d_{12}(70) ^{13}C CP MAS (C), ^{31}P CP MAS (D), and ^{31}P SPE (E).

weak peak at 33.6 ppm, characteristic of an inclusion complex, the ^{31}P CP MAS spectrum of the inclusion contains additional peaks at 12.5, −2.1, and −21.1 ppm. The ^{31}P SPE NMR spectrum of the same sample is dominated by the three resonances characteristic of monoclinic TPP.

X-ray Powder Diffraction. The inclusion compounds **1**@TPP-d_{12} to **3**@TPP-d_{12} were characterized by Cu Kα1 wavelength X-ray powder patterns. As an example, Figure 7 shows the powder pattern for 5%**1**@TPP-d_{12}(70) plotted as X-ray photon counts versus the scattering wave vector magnitude q, where q is related to the scattering angle θ and X-ray wavelength λ by $q = (4\pi/\lambda)\sin\theta$. The large peaks in the pattern arise from a hexagonal inclusion phase with an in-plane lattice parameter of 1.168 ± 0.001 nm and hexagonal layer spacing of 0.990 ± 0.001 nm. The in-plane lattice parameter and layer spacing show roughly 2.5% expansion and 1.7% contraction, respectively, compared to the 1.1454 ± 0.0005 nm and 1.0160 ± 0.0005 nm reported[42] for empty hexagonal TPP. Peak widths allow us to estimate the typical powder particle size at near 300 nm. In addition to peaks associated with the hexagonal phase, we find additional small peaks that arise from the monoclinic phase of TPP.

In 5%**1**@TPP-d_{12}(235), the TPP monoclinic diffraction peaks are absent, and the hexagonal peaks are narrower,

DOI: 10.1021/acs.joc.5b00661
J. Org. Chem. 2015, 80, 6173−6192

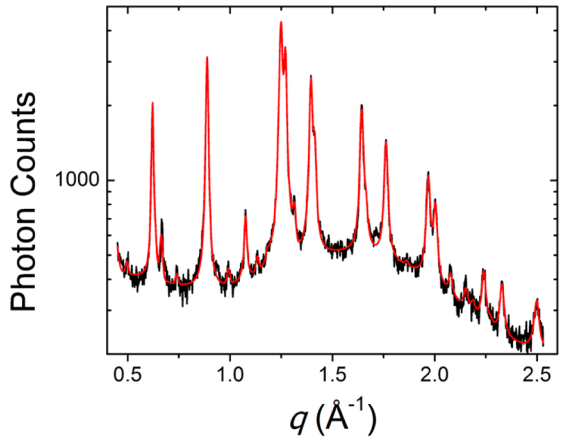

Figure 7. X-ray powder pattern for 5%**1**@TPP-d_{12}(70). The solid black line is the diffraction data, and the red line is the fit assuming hexagonal peak positions and a measured background from the sample capillary tube.

which is consistent with an increase in powder particle size. The in-plane hexagonal lattice parameter is now 1.167 ± 0.001 nm, and the hexagonal layer spacing is 0.982 ± 0.001 nm. XRD powder patterns of the 5%**2**@TPP-d_{12}(70) and 5%**3**@TPP-d_{12}(70) samples show a mixture of hexagonal and monoclinic TPP. The hexagonal lattice parameters are consistent with those of empty TPP.

In the XRD pattern of 5%**2**@TPP-d_{12}(235), peaks of monoclinic TPP are absent. It contains signals from a hexagonal inclusion phase with an in-plane lattice parameter of 1.166 ± 0.001 nm, layer spacing of 0.996 ± 0.001 nm, and many small unassigned peaks.

The XRD powder pattern of 16%**2**@TPP-d_{12}(70) shows a mixture of monoclinic TPP and a hexagonal inclusion compound with an in-plane lattice parameter of 1.164 ± 0.001 nm and layer spacing of 0.999 ± 0.001 nm. Annealing this sample to 235 °C resulted in the elimination of all significant diffraction peaks and apparent decomposition of the sample.

Dielectric Spectroscopy. Dielectric loss peaks at low temperatures are indications of dielectric relaxations related to rotations of dipolar rotators. The rotational barrier and attempt frequency of a rotational mode can be extracted by analyzing the positions of the associated dielectric loss peaks for different external field frequencies.

Two major dielectric loss peaks in the 100−200 K range that disperse with frequency are seen for 5%**1**@TPP-d_{12}(70) (Figure 8). A peak near 100 K is consistent with a rotational mode with a barrier of 3.98 kcal/mol and an attempt frequency of 7.5 × 10^{11} Hz. The other, between 150 and 200 K, is consistent with a barrier of 9.64 kcal/mol and an attempt frequency of 9.6 × 10^{16} Hz. There also is a small dielectric loss shoulder below 100 K, representing a rotation with a barrier of 2.39 kcal/mol and an attempt frequency of ∼8 × 10^{10} Hz.

Upon going to 5%**1**@TPP-d_{12}(235), one of the two major peaks in the dielectric loss spectrum between 80 K and room temperature is shifted to higher temperature (Figure 9). The barrier height of the lower peak increases slightly from 3.98 to 4.36 kcal/mol with an almost unchanged attempt frequency. The peak is now much smaller, suggesting a reduced population of rotators active in this rotational mode.

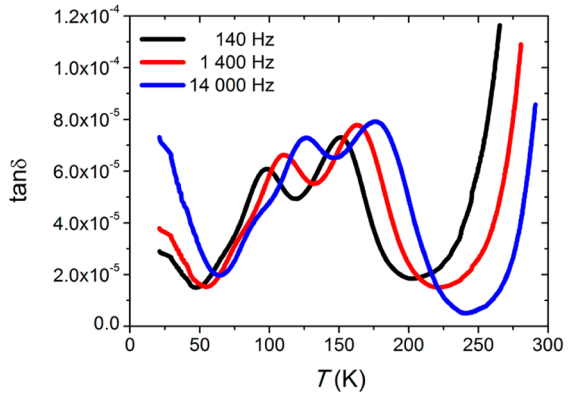

Figure 8. Dielectric loss of 5%**1**@TPP-d_{12}(70) between 10 and 280 K. Black, 140 Hz; red, 1400 Hz; blue, 14000 Hz.

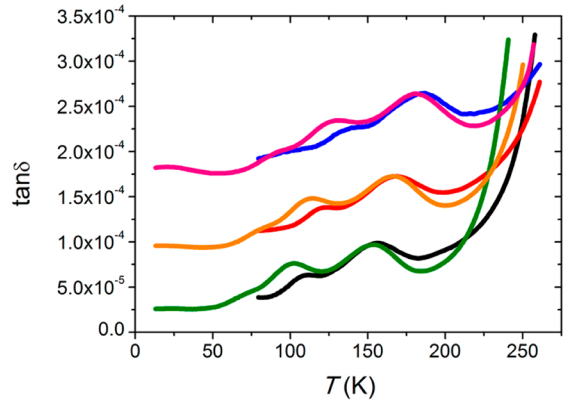

Figure 9. Dielectric loss of 5%**1**@TPP-d_{12}(70) at 140 Hz (green), 1400 Hz (orange), and 14000 Hz (purple), and 5%**1**@TPP-d_{12}(235) at 140 Hz (black), 1400 Hz (red), and 14000 Hz (blue). The curves have been shifted vertically for better viewing.

16%**2**@TPP-d_{12}(70) also has two frequency-dispersing dielectric loss peaks between 50 and 150 K (Figure 10). One

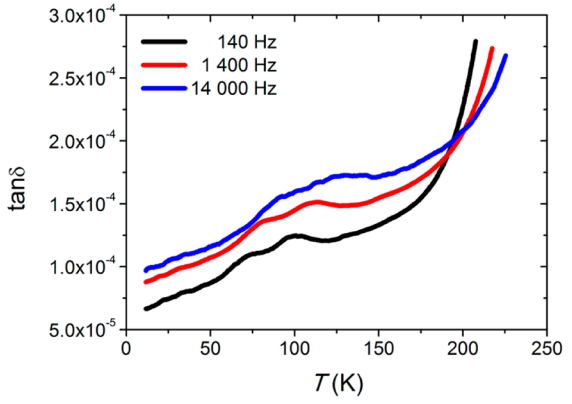

Figure 10. Dielectric loss of 16%**2**@TPP-d_{12}(70) in the range 10−220 K at 140 Hz (black), 1400 Hz (red), and 14000 Hz (blue).

is consistent with a rotational mode with a barrier of 3.43 kcal/mol and an attempt frequency of 2.2 × 10^{13} Hz. The other has a barrier of 4.38 kcal/mol and an attempt frequency of 5 × 10^{12} Hz. Both peaks are much smaller than the major peaks of 5%**1**@TPP-d_{12}(70), indicating that far fewer rotators are active.

DOI: 10.1021/acs.joc.5b00661
J. Org. Chem. 2015, 80, 6173−6192

The dielectric spectrum of 5%**3**@TPP-d_{12}(70) is relatively featureless in the temperature range of interest, suggesting that either too few rotators can actually rotate or that rotational barriers are so high that possible dielectric loss peaks lie at high temperatures (Figure 11).

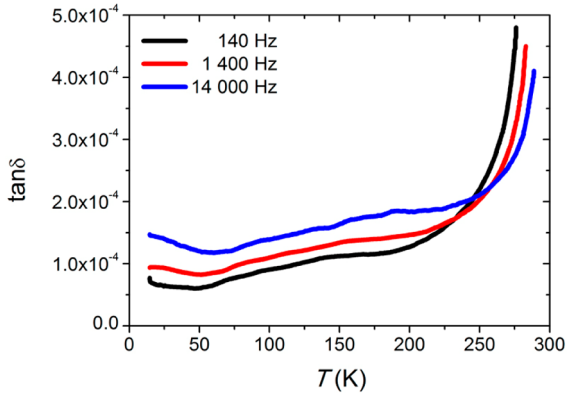

Figure 11. Dielectric loss of 5%**3**@TPP-d_{12}(70) between 10 and 280 K at 140 Hz (black), 1400 Hz (red), and 14000 Hz (blue).

DISCUSSION

Synthesis. The design concept for a multistep synthesis of the molecular rotors **1**−**3** based on the preparation of two key molecular fragments whose coupling produces the target rotors in the final step worked as we had hoped. This strategy allows their preparation on a scale of hundreds of milligrams. The generality of this approach is apparent, because singly protected alkyne **19** could in principle be coupled with almost any (hetero)aryl bromide, iodide, or triflate, providing access to a variety of dipolar rotators.

The only other observation that requires comment is the low chemical stability of the $Si(TMS)_3$ group relative to TMS (Scheme 9). The reaction of **39** with MeLi in THF at −78 °C demonstrated that the bulky and electron-poor $Si(TMS)_3$ group could be selectively cleaved in the presence of TMS in a nearly quantitative isolated yield.

Inclusion Compounds. The production of inclusion compounds by milling proceeded as usual. The only novelty is high temperature annealing, which provided access to samples that contained only the hexagonal form of TPP.

The X-ray powder patterns indicate that both **1** and **2** form hexagonal inclusion compounds with TPP, whereas symmetrical compound **3** does not. The nearly identical hexagonal lattice parameters that we find for inclusion compounds of both **1** and **2** are entirely consistent with their identical tail structure and thus with our picture of how these rotor molecules form surface inclusions on TPP.

Rotor 1. The carbon atoms present in the *tert*-butyl moiety, the bicyclo[1.1.1]pentane cage, and the triptycene unit appear slightly shifted in the ^{13}C CP MAS NMR spectrum of the inclusion compounds. The doubling of the signal of the bridge carbons of bicyclo[1.1.1]pentane proves the existence of two distinct environments for this part of the shaft, present at equilibrium in approximately the same amounts and unchanged by additional annealing. It is also compatible with the possible doubling of the signal of the methyl carbons of the *tert*-butyl group. The bridgehead carbons of triptycene produce a signal at 53.7 ppm, only 0.4 ppm from their location in solution. We conclude that all of the rods have their triptycenes outside the channel and their shafts inserted, one-half of them deeper than the other. Given the trigonal arrangement of the channels, the insertion pattern cannot be completely regular but we have no other information on it.

The signal near 78 ppm in the solid-state NMR spectrum can be assigned to all of the acetylenic carbon atoms present in **1**.

The only peak observed in the ^{31}P CP MAS spectrum of 5%**1**@TPP-d_{12}(70) is indicative of an inclusion in the TPP channel. However, the peaks corresponding to the monoclinic TPP observed in the ^{31}P SPE NMR spectrum suggest that 5% loading of rotor **1** was not optimal and that ∼25% of the TPP collapsed from the hexagonal form to the monoclinic one.

The analysis of 5%**1**@TPP-d_{12}(235) provided three important pieces of information: (i) rotor **1** survives the high temperature as revealed by ^{13}C CP MAS NMR, (ii) on the basis of the ^{31}P SPE NMR, the TPP is present almost exclusively in its hexagonal form, and (iii) a significant amount of phosphorus-containing TPP decomposition products were formed (^{31}P CP MAS NMR and ^{13}C CP MAS NMR). It is not clear whether these decomposed structures were formed by degradation of hexagonal TPP or its monoclinic modification, which was originally present in the sample.

Rotor 2. From the solid state NMR spectrum of 5%**2**@TPP-d_{12}(70) in Figure S2 (Supporting Information), it is obvious that the general procedure for the preparation of inclusions does not produce a pure hexagonal inclusion of rotor **2**. Although the ^{31}P SPE NMR spectrum indicates that there is still some free hexagonal TPP in the system, the ^{31}P CP MAS spectrum suggests the existence of an inclusion in the TPP channel.

The ^{13}C CP MAS NMR spectrum of 5%**2**@TPP-d_{12}(70) is very similar to that of 5%**1**@TPP-d_{12}(70) but contains additional unresolved peaks attributable to the trimethyladamantyl moiety. The signal of the bridge carbons of the bicyclo[1.1.1]pentane cage again appears as a doublet of peaks of similar intensity at 60.7 and 57.3 ppm, the same locations as in 5%**1**@TPP-d_{12}(70). The signal of the methyls of the *tert*-butyl group also appears as an upfield shifted doublet but is so strongly overlapped with signals of adamantyl carbons that it does not allow for any firm conclusions. The signals of the triptycene bridgeheads again exhibit a minimal shift (0.3 ppm) from their position in solution. The peak corresponding to the proximal methylene groups in the adamantyl substituent appears at the same chemical shift in all of the spectra (48.7 ppm in solution and 48.9 ppm in the solids), nicely compatible with the notion that the bulky trimethyladamantyl is not inserted in the channel.

The signal at 75 ppm in the solid-state NMR spectrum can be assigned to all of the acetylenic carbon atoms present in rotor **2**.

The ^{13}C CP MAS NMR spectra of 16%**2**@TPP-d_{12}(70) and 16%**2**@TPP-d_{12}(235) are very similar to that of 5%**2**@TPP-d_{12}(70). The ^{31}P SPE NMR spectrum of 16%**2**@TPP-d_{12}(70) shows almost exclusively hexagonal TPP, and its ^{31}P CP MAS NMR spectrum reveals the presence of a minor decomposition product of TPP. Both ^{31}P NMR spectra of 16%**2**@TPP-d_{12}(235) show extensive decomposition of TPP.

Overall, we conclude that the rods of **2** form a surface and not a bulk inclusion, and that half of them are inserted deeper than that other half. Only the shaft part of the rotor molecule, separated from the rotator by the triptycene stopper, is capable of insertion. The surface inclusions of **2** are very similar to those of **1**, and both rotors are thermally very stable. For

DOI: 10.1021/acs.joc.5b00661
J. Org. Chem. 2015, 80, 6173−6192

reasons that are unclear, the TPP constituent is thermally less stable in the former.

Rotor 3. The solid-state ^{13}C CP MAS NMR spectra of 5%**3**@TPP-d_{12}(70) are almost identical to those of neat solid rotor **3**. The signals of TPP are detectable but very weak, indicating that only very little magnetization is transmitted from proton containing moieties to the carbon atoms of TPP-d_{12}. Judging by the ^{31}P SPE NMR spectrum, the content of monoclinic TPP in the inclusion sample is almost 85%. The very weak ^{31}P CP MAS signal again shows that no part of rotor **3** is included in the channel.

Rotational Barriers. The dielectric spectra of **1**@TPP-d_{12} and **2**@TPP-d_{12} indicate that rotators can rotate with barriers as low as 3−4 kcal/mol, and a small fraction may have an even lower barrier in the 2 kcal/mol range. The sizes of the dielectric loss peaks of **1**@TPP-d_{12} are comparable to other surface inclusions in TPP,[10] which is consistent with the conclusion of solid-state NMR and XRD studies that a surface inclusion has been formed. Given that half of the rotors **1** and **2** are inserted deeper than the other half, it is easy to see why the surface inclusion of **2** contains far fewer active rotators than that of **1**. Instead of keeping the rotor axles apart as intended, the trimethyladamantyl groups block the rotators of their differently inserted molecular rotor neighbors (Figure 12). It is likely

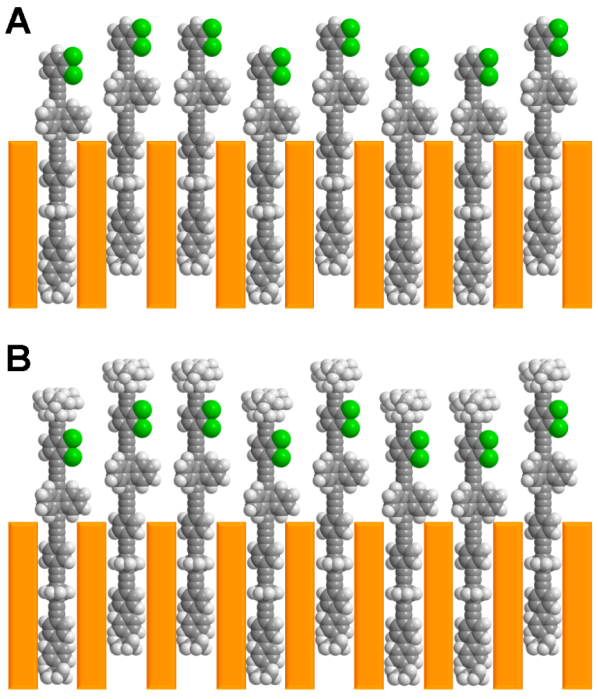

Figure 12. Side views of proposed structures of surface inclusions **1**@TPP-d_{12} (A) and **2**@TPP-d_{12} (B).

that many neighbor pairs are packed similarly to those in the single crystals of the triptycene derivatives shown in Figure 3. The same structural feature is likely responsible for the differences between the rotational barriers observed in the two inclusion compounds, particularly the absence of the 9.64 kcal/mol barrier in the inclusion compounds of **2**. Rotor **3** did not form an inclusion with TPP; thus, the absence of dielectric losses in **3**@TPP-d_{12} spectrum is expected.

No ferroelectricity is observed at low temperatures, probably because the barriers to rotation are excessive and, probably more importantly, because the rotating dipoles are not all located in the same plane.

CONCLUSIONS

The triptycene unit works well as a stopper in TPP channels, the NMR markers perform as desired, the dichlorophenyl rotator and the trimethyladamantyl substituent are bulky enough to prevent undesired backward insertion of the rotor into the TPP channel, and both compounds **1** and **2** form surface inclusions in TPP as intended. However, in these inclusions, half of the rods are inserted deeper than the other half, apparently imitating the packing found in single crystals of **16**, **17**, and **20**, and likely to be present in the crystals of neat rotors. The resulting staggering of the rods is probably responsible for the relatively high observed rotational barriers of 3.98 and 9.64 kcal/mol for 5%**1**@TPP-d_{12} and 3.43 and 4.38 kcal/mol for 16%**2**@TPP-d_{12}as well as the absence of ferroelectricity. As expected, the presence of the two bulky 1,2-dichlorophenyl groups (whose diameter is larger than the internal diameter of the TPP channel) in symmetrical molecular rotor **3** prevents its insertion into the TPP channel.

To achieve a ferroelectric ground state, it would be helpful to force all guest rotors to penetrate the TPP channels to the same depth, perhaps by providing the triptycene stoppers with six peripheral substituents that have high affinity for their counterparts on neighboring triptycenes, or by modifying the bulky terminal moieties in a way that would provide them with affinity for their bulky neighbors, or both. The use of a hexahalotriptycene as a stopper and C_{60} as a terminal group may be worth exploring. Using the shorter ethynylene instead of butadiynylene axles would likely be another improvement.

EXPERIMENTAL SECTION

Materials. All reactions were carried out under an argon atmosphere with dry solvents freshly distilled under anhydrous conditions unless otherwise noted. Standard Schlenk and vacuum line techniques were employed for all manipulations with air- or moisture-sensitive compounds. Yields refer to isolated chromatographically and spectroscopically homogeneous materials unless otherwise stated.

THF and ether were dried over sodium with benzophenone and distilled under argon prior to use. Triethylamine and CH_2Cl_2 were dried over CaH_2 and distilled under argon prior to use. All other reagents were used as supplied unless otherwise stated.

Analytical thin-layer chromatography (TLC) was performed using precoated TLC aluminum sheets (Silica gel 60 F_{254}). Spots on TLC were visualized using either UV light (254 nm) or a 5% solution of phosphomolybdic acid in ethanol using heat (200 °C) as a developing agent. Flash chromatography was performed using silica gel (high purity grade, pore size 60 Å, 70−230 mesh). Melting points reported are uncorrected. Infrared spectra (IR) were recorded in KBr pellets. NMR chemical shifts are reported relative to $CHCl_3$ (δ = 7.26 ppm for ^1H NMR), $CHCl_3$ (δ = 77.0 ppm for ^{13}C NMR), THF-d_8 (δ = 1.72 and 3.58 ppm for ^1H NMR), THF-d_8 (δ = 25.40 and 67.50 ppm for ^{13}C NMR), acetone-d_6 (δ = 2.05 ppm for ^1H NMR), and acetone-d_6 (δ = 29.8 and 206.3 ppm for ^{13}C NMR) as internal references. Splitting patterns are assigned as s = singlet, d = doublet, t = triplet, m = multiplet, and br = broad signal.

High-resolution mass spectra (HRMS) using atmospheric pressure chemical ionization (APCI) and electrospray ionization (ESI) were obtained on a mass analyzer combining linear ion trap and the Orbitrap, and those using electron ionization (EI) and chemical ionization (CI) mode were taken on a time-of-flight mass spectrometer.

DOI: 10.1021/acs.joc.5b00661
J. Org. Chem. 2015, 80, 6173−6192

TPP-d_{12} was synthesized from catechol-d_6[43] as reported.[44] The code for designating an inclusion compound is X%**Y**@TPP-d_{12}(T), where X is the molar percentage of rotor Y, and T is the annealing temperature.

The previously published procedure[15] for preparing the inclusion compounds from components was modified as follows. The neat rotors **1**−**3** and neat solvent-free hexagonal TPP-d_{12} were mixed, ball milled for 2 h with a stainless steel disk, and annealed for 2 days at 70 °C under an argon atmosphere. Some samples were annealed for two more minutes at 235 °C.

Single-Crystal X-ray Diffraction. Crystallographic data for **16**, **17**, **20**, and **26** were collected on a Kappa geometry diffractometer with a CCD detector by monochromatized Mo Kα radiation (λ = 0.71073 Å) at a temperature of 150(2) K. The structures were solved by direct methods (SHELXS)[45] and refined by full matrix least-squares based on F^2 (SHELXL97).[45]

X-ray Powder Diffraction. The X-ray powder patterns were taken with a system based on a Rigaku Ultrax18 rotating anode generator. It uses a curved silicon multilayer monochromator to produce Cu Kα radiation at a wavelength of λ = 0.15418 nm. Powder samples, loaded into 1.0 mm diameter borosilicate glass capillaries with a wall thickness of 10 μm, were mounted on a Huber four-circle goniometer. The scattered X-rays were measured with a NaI scintillator point detector that was moved in a horizontal plane by an angle 2θ with respect to the direction of the incident X-rays to scan the Bragg scattering profile. The resolution of the instrument, in its usual configuration, is $q_{res} \approx 0.003$ Å^{-1}.

Dielectric Spectroscopy. The powder samples were loaded onto the surface of coplanar interdigitated electrode capacitators fabricated by gold metallization on fused silica substrates (each with 50 fingers separated by ~10 μm gaps). Nominal capacitor values for the empty capacitors were near 1 pF and dielectric loss tangents were at or below 10^{-15} level. An Andeen−Hagerling capacitance bridge was used to measure the dielectric loss and capacitance with sinusoidal alternating voltage (1.8−5 V and 0.12−12 kHz) applied on the capacitor. Data were taken continuously with the temperature slowly changing between 7 K and room temperature. The curves were averaged over heating and cooling steps and smoothed.

Synthesis. Rotor 1. A flame-dried Schlenk flask was charged with **5** (150 mg, 0.303 mmol), **4** (153 mg, 0.290 mmol), $Pd(PPh_3)_4$ (14 mg; 0.012 mmol, 4 mol %), and CuI (2 mg, 0.009 mmol, 3 mol %). After three successive vacuum/argon cycles, degassed dry THF (15 mL) and triethylamine (8 mL) were added from a syringe. The yellow solution was stirred for 16 h at room temperature. A dense white solid precipitated. The crude reaction mixture was centrifugated to remove solvents (10 min, 3000 rpm). The white solid residue was placed on a frit and washed with 10% aq HCl (2 × 10 mL), concentrated aq NH_4Cl (2 × 10 mL), water (3 × 10 mL), hexane (4 × 20 mL), $CHCl_3$ (2 × 10 mL), and ether (2 × 5 mL) and finally dried using a Kugelrohr distillation apparatus (60 min, 80 °C, 500 mTorr). Molecular rotor **1** was obtained as a white crystalline solid (196 mg, 0.219 mmol, 76%).

Mp >320 °C (dec.). ^{1}H NMR (500 MHz, THF-d_8): δ 1.34 (s, 9H), 2.46 (s, 6H), 7.14−7.17 (m, 6H), 7.38 (dd, J_1 = 7.72 Hz, J_2 = 8.13 Hz, 1H), 7.42−7.43 (m, 2H), 7.45−7.47 (m, 4H), 7.55−7.56 (m, 2H), 7.57−7.59 (m, 2H), 7.63−7.65 (m, 2H), 7.66 (dd, J_1 = 1.48 Hz, J_2 = 8.13 Hz, 1H), 7.72−7.76 (m, 7H). ^{13}C NMR (125 MHz, THF-d_8): δ 31.7, 32.0, 35.3, 54.1, 59.8, 75.4, 75.5, 77.4, 77.9, 78.7, 79.2, 79.3, 80.3, 80.4, 81.0, 89.1, 92.0, 121.8, 122.6, 123.05, 123.11, 124.5, 125.7, 126.6, 127.12, 127.13, 127.3, 127.4, 129.0, 132.83, 132.85, 132.93, 133.6, 134.2, 134.3, 135.9, 138.2, 141.7, 143.8, 144.0, 151.4. IR (KBr): 3069, 3033, 3016, 2988, 2963, 2913, 2876, 2221, 2152, 1607, 1577, 1551, 1494, 1472, 1459, 1453, 1407, 1394, 1362, 1341, 1303, 1267, 1212, 1191, 1174, 1155, 1141, 1113, 1102, 1049, 1033, 1013, 1003, 979, 948, 921, 873, 852, 837, 820, 781, 750, 722, 706, 677, 653, 647, 639, 567, 544, 525, 491, 476 cm^{-1}. MS m/z (%): 893.3 (100, M + H). HRMS (APCI) for ($C_{65}H_{42}Cl_2$ + H^+): calcd, 893.27363; found, 893.27388. Anal. Calcd for $C_{65}H_{42}Cl_2$: C, 87.33; H, 4.74. Found: C, 87.28; H, 4.87.

Rotor 2. The procedure for **1** was followed starting with **6** (150 mg, 0.216 mmol), **4** (111 mg, 0.210 mmol), $Pd(PPh_3)_4$ (10 mg, 0.009 mmol, 4 mol %), and CuI (1 mg, 0.006 mmol, 3 mol %) in dry and degassed THF (8 mL) and triethylamine (8 mL). Molecular rotor **2** was obtained as a white crystalline solid (160 mg, 0.146 mmol, 70%).

Mp >260 °C (dec.). ^{1}H NMR (500 MHz, $CDCl_3$): δ 0.89 (s, 9H), 1.09−1.12 (m, 3H), 1.17−1.20 (m, 3H), 1.35 (s, 9H), 1.58 (s, 6H), 2.47 (s, 6H), 7.15−7.17 (m, 6H), 7.42−7.44 (m, 2H), 7.44 (d, J = 8.05 Hz, 1H), 7.46−7.47 (m, 4H), 7.55−7.57 (m, 2H), 7.58−7.59 (m, 2H), 7.63−7.65 (m, 2H), 7.67 (d, J = 8.06 Hz, 1H), 7.73−7.74 (m, 6H). ^{13}C NMR (125 MHz, $CDCl_3$): δ 30.4, 31.7, 32.0, 32.5, 34.0, 35.3, 48.7, 50.7, 54.17, 54.19, 59.8, 75.50, 75.54, 77.42, 77.44, 77.9, 78.7, 79.2, 80.2, 80.4, 80.9, 81.1, 89.1, 92.0, 107.9, 121.8, 122.7, 123.06, 123.13, 125.7, 126.6, 127.13, 127.14, 127.3, 127.5, 128.1, 132.0, 132.86, 132.94, 133.2, 133.6, 135.7, 136.5, 138.2, 141.7, 143.8, 144.0, 151.5. IR (KBr): 3069, 3033, 3017, 2945, 2915, 2891, 2862, 2840, 2225, 1607, 1580, 1494, 1453, 1403, 1394, 1364, 1353, 1303, 1267, 1253, 1210, 1154, 1141, 1113, 1102, 1032, 1013, 1004, 981, 964, 946, 926, 874, 852, 836, 821, 752, 723, 660, 647, 639, 608, 573, 544, 507, 492, 478 cm^{-1}. MS m/z (%): 1093.4 (100, M + H). HRMS (APCI) for ($C_{80}H_{62}Cl_2$ + H^+): calcd 1093.43013, found 1093.43026. Anal. Calcd for $C_{80}H_{62}Cl_2$: C, 87.81; H, 5.71. Found: C, 87.71; H, 5.85.

9,10-Bis[2,3-dichlorophenylbuta-1,3-diynyl]triptycene (3). A flame-dried Schlenk flask was charged with **20** (60 mg, 0.171 mmol), 1,2-dichloro-3-iodobenzene (**27**) (98 mg, 0.359 mmol), $Pd(PPh_3)_4$ (16 mg; 0.014 mmol, 8 mol %), and CuI (2 mg, 0.010 mmol, 6 mol %). After three successive vacuum/argon cycles, dry and degassed THF (5 mL) and triethylamine (5 mL) were added from a syringe. The slightly yellowish solution was stirred for 18 h at room temperature. A dense white solid precipitated. The crude reaction mixture was diluted with CH_2Cl_2 (100 mL), washed with saturated aq NH_4Cl (2 × 20 mL), and dried over $MgSO_4$. Column chromatography on silica gel (hexane/CH_2Cl_2 = 4:1) yielded **3** as a white crystalline solid (86 mg, 0.134 mmol, 78%).

Mp >315 °C (dec.). ^{1}H NMR (400 MHz, $CDCl_3$): δ 7.15−7.17 (m, 6H), 7.25 (dd, J_1 = 7.65 Hz, J_2 = 8.19 Hz, 2H), 7.53 (dd, J_1 = 1.47 Hz, J_2 = 8.10 Hz, 2H), 7.62 (dd, J_1 = 1.47 Hz, J_2 = 7.74 Hz, 2H), 7.78−7.80 (m, 6H). ^{13}C NMR (100 MHz, $CDCl_3$): δ 53.1, 74.5, 76.5, 78.9, 79.4, 122.4, 123.8, 126.1, 127.2, 131.4, 132.8, 133.7, 135.5, 142.7. IR (KBr): 3075, 3061, 3034, 3016, 2954, 2925, 2853, 2243, 2161, 1607, 1577, 1551, 1452, 1412, 1407, 1339, 1303, 1261, 1220, 1191, 1156, 1142, 1112, 1077, 1049, 1032, 983, 949, 842, 796, 782, 749, 703, 639, 570, 530, 491, 474, 455 cm^{-1}. MS m/z (%): 641.1 (100, M + H, center of isotope cluster). HRMS (APCI) for ($C_{40}H_{18}Cl_4$ + H^+): calcd 639.0235, found 639.0226. Anal. Calcd for $C_{40}H_{18}Cl_4$: C, 75.02; H, 2.83. Found: C, 74.98; H, 3.22.

1-((4′-*tert*-Butylbiphenyl-4-yl)ethynyl)-3-((4-iodophenyl)-ethynyl)bicyclo[1.1.1]pentane (4). The procedure for **3** was followed starting with **10** (200 mg, 0.616 mmol), 1,4-diiodobenzene (1.017 g, 3.082 mmol, 5 equiv), $Pd(PPh_3)_4$ (29 mg, 0.025 mmol, 4 mol %), and CuI (4 mg, 0.018 mmol, 3 mol %) in dry and degassed THF (20 mL) and triethylamine (5 mL). Column chromatography on silica gel (hexane/CH_2Cl_2 = 4:1, then hexane/CH_2Cl_2 = 1:1) gave **4** as a white crystalline solid (252 mg, 0.479 mmol, 78%).

Mp >275 °C (dec.). ^{1}H NMR (400 MHz, $CDCl_3$): δ 1.36 (s, 9H), 2.48 (s, 6H), 7.12−7.14 (m, 2H), 7.45−7.47 (m, 4H), 7.51−7.54 (m, 4H), 7.62−7.64 (m, 2H). ^{13}C NMR (100 MHz, $CDCl_3$): δ 30.7, 31.0, 31.3, 34.6, 59.0, 79.2, 80.1, 88.6, 89.7, 94.0, 121.4, 122.4, 125.8, 126.6, 126.7, 132.1, 133.3, 137.3, 137.4, 140.6, 150.7. IR (KBr): 2986, 2969, 2952, 2907, 2871, 2221, 1494, 1482, 1476, 1445, 1394, 1388, 1366, 1359, 1297, 1280, 1269, 1212, 1201, 1116, 1055, 1031, 1005, 854, 823, 785, 747, 742, 723, 574, 546, 530 cm^{-1}. MS m/z (%): 527.1 (100, M + H). HRMS (APCI) for ($C_{31}H_{27}I$ + H^+): calcd 527.12302, found 527.12297. Anal. Calcd for $C_{31}H_{27}I$: C, 70.72; H, 5.17. Found: C, 70.64; H, 5.17.

9-((2,3-Dichlorophenyl)buta-1,3-diynyl)-10-(buta-1,3-diynyl)triptycene (5). A solution of TBAF in THF (1.0 M, 0.50 mL, 0.500 mmol) was added to a stirred solution of **28** (236 mg, 0.416 mmol) in wet THF (10 mL) at room temperature. The reddish reaction mixture was stirred at that temperature for 30 min. The mixture was then diluted with ether (60 mL), washed with water (2 × 20 mL), and the organic phase was dried over $MgSO_4$. Solvents were removed under reduced pressure and column chromatography on

DOI: 10.1021/acs.joc.5b00661
J. Org. Chem. 2015, 80, 6173−6192

silica gel (hexane/CH_2Cl_2 = 4:1) afforded **5** as a white crystalline solid (200 mg, 0.404 mmol, 97%).

Mp >210 °C (dec.). ^{1}H NMR (400 MHz, $CDCl_3$): δ 3.30 (s, 1H), 7.13−7.15 (m, 6H), 7.36 (dd, J_1 = 7.64 Hz, J_2 = 8.18 Hz, 1H), 7.65 (dd, J_1 = 1.45 Hz, J_2 = 8.13 Hz, 1H), 7.69−7.75 (m, 7H). ^{13}C NMR (100 MHz, $CDCl_3$): δ 53.7, 54.1, 67.9, 71.1, 71.6, 75.4, 77.4, 77.9, 79.3, 80.3, 123.01, 123.03, 124.5, 127.10, 127.12, 128.9, 132.8, 134.2, 134.4, 135.9, 143.78, 143.82. IR (KBr): 3298, 3069, 3034, 3015, 2955, 2927, 2869, 2241, 2223, 2162, 2068, 1608, 1579, 1551, 1530, 1454, 1414, 1410, 1340, 1302, 1256, 1228, 1197, 1155, 1141, 1120, 1107, 1078, 1050, 1034, 982, 971, 965, 948, 922, 905, 884, 874, 858, 783, 756, 751, 736, 706, 700, 668, 639, 622, 567, 554, 521, 497, 483, 478, 454 cm^{-1}. MS m/z (%): 495.1 (100, M + H). HRMS (APCI) for ($C_{34}H_{16}Cl_2$ + H^+): calcd 495.07018, found 495.07013. Anal. Calcd for $C_{34}H_{16}Cl_2$: C, 82.43; H, 3.26. Found: C, 82.42; H, 3.44.

Compound 6. The procedure for **5** was followed starting with **29** (200 mg, 0.260 mmol) in wet THF (8 mL) and a solution of TBAF in THF (1.0 M, 313 μL, 0.313 mmol). Column chromatography on silica gel (hexane/CH_2Cl_2 = 6:1) afforded **6** as a white crystalline solid (176 mg, 0.253 mmol, 97%).

Mp >200 °C (dec.). ^{1}H NMR (500 MHz, $CDCl_3$): δ 0.89 (s, 9H), 1.08−1.10 (m, 3H), 1.16−1.18 (m, 3H), 1.57 (s, 6H), 2.43 (s, 1H), 7.13−7.15 (m, 6H), 7.34 (d, J = 8.10 Hz, 1H), 7.50 (d, J = 8.10 Hz, 1H), 7.72−7.78 (m, 6H). ^{13}C NMR (125 MHz, $CDCl_3$): δ 29.9, 31.7, 32.9, 47.8, 49.9, 52.6, 53.1, 67.6, 68.6, 71.1, 74.7, 76.5, 76.6, 77.2, 79.6, 79.8, 107.1, 122.0, 122.3, 122.4, 126.10, 126.12, 126.9, 130.6, 131.6, 135.2, 135.9, 142.6, 142.7. IR (KBr): 3310, 3291, 3069, 3034, 2943, 2917, 2890, 2861, 2837, 2226, 1607, 1580, 1453, 1367, 1353, 1303, 1253, 1225, 1154, 1142, 1110, 1032, 1003, 984, 967, 926, 909, 831, 752, 733, 639, 616, 559, 549, 526, 495, 478 cm^{-1}. MS m/z (%): 695.2 (100, M + H). HRMS (APCI) for ($C_{49}H_{36}Cl_2$ + H^+): calcd 695.22668, found 695.22675. Anal. Calcd for $C_{49}H_{36}Cl_2$ + $CDCl_3$ in a 3:2 ratio: C, 76.94; H, 4.77. Found: C, 76.64; H, 4.86.

4-Bromo-4′-*tert*-butylbiphenyl (7).[29] A previously published procedure[29] was adapted as follows: To a solution of 4-bromobiphenyl (5.00 g, 21.450 mmol) and *tert*-BuCl (2.39 mL, 22.000 mmol) in dry CCl_4 (30 mL) was added freshly sublimed $AlCl_3$ (267 mg, 2.000 mmol) at 0 °C. The reaction mixture was stirred for an additional 60 min at 0 °C. The solution turned green immediately and massive evolution of gaseous HCl was observed. The reaction mixture was diluted with $CHCl_3$ (100 mL), washed with saturated aq $NaHCO_3$ (3 × 20 mL) and water (3 × 20 mL), and finally dried over $MgSO_4$. Solvents were removed under reduced pressure, and a yellowish solid residue was recrystallized from methanol. Crystals were filtered on a frit, washed with cold methanol (2 × 20 mL), and dried under reduced pressure (500 mTorr, 50 °C, 60 min). Compound **7** was obtained as a white crystalline solid (4.214 g, 14.570 mmol, 68%).

^{1}H NMR (400 MHz, $CDCl_3$): δ 1.37 (s, 9H), 7.45−7.52 (m, 6H), 7.54−7.56 (m, 2H). ^{13}C NMR (100 MHz, $CDCl_3$): δ 31.3, 34.5, 121.1, 125.8, 126.4, 128.5, 131.8, 137.0, 139.9, 150.7, which is in agreement with the literature.[29]

((3-((4′-*tert*-Butylbiphenyl-4-yl)ethynyl)bicyclo[1.1.1]pent-1-yl)ethynyl)trimethylsilane (9). A flame-dried Schlenk flask was charged with **8**[30,31] (540 mg, 2.867 mmol), **7** (995 mg, 3.441 mmol), $Pd(PPh_3)_4$ (133 mg, 0.115 mmol, 4 mol %), and CuI (16 mg, 0.086 mmol, 3 mol %). After three successive vacuum/argon cycles, dry and degassed THF (10 mL) and triethylamine (5 mL) were added from a syringe. The yellow solution was stirred for 20 h at 55 °C. A dense white solid precipitated. The crude reaction mixture was diluted with CH_2Cl_2 (150 mL), washed with saturated aq NH_4Cl (2 × 30 mL), and the clear yellow organic phase was dried over $MgSO_4$. Column chromatography on silica gel (hexane/CH_2Cl_2 = 4:1) gave **9** as a white crystalline solid (906 mg, 2.284 mmol, 80%).

Mp 268.4−269.9 °C. ^{1}H NMR (400 MHz, $CDCl_3$): δ 0.16 (s, 9H), 1.35 (s, 9H), 2.41 (s, 6H), 7.44−7.47 (m, 4H), 7.50−7.53 (m, 4H). ^{13}C NMR (100 MHz, $CDCl_3$): δ 0.0, 30.6, 30.7, 31.3, 34.6, 59.0, 79.9, 84.7, 88.8, 104.6, 121.4, 125.8, 126.6, 126.7, 132.1, 137.3, 140.6, 150.7. IR (KBr): 3032, 2990, 2963, 2913, 2876, 2165, 1604, 1493, 1477, 1462, 1446, 1394, 1362, 1318, 1264, 1254, 1201, 1180, 1113, 1082, 1027, 1003, 920, 857, 843, 822, 760, 743, 723, 699, 621, 572, 545, 532 cm^{-1}. MS m/z (%): 419.2 (100, M + Na), 397.2 (42, M + H). HRMS (ESI+) for ($C_{28}H_{32}Si$ + H^+): calcd 397.23460, found 397.23461. Anal. Calcd for $C_{28}H_{32}Si$: C, 84.79; H, 8.13. Found: C, 84.49; H, 7.96.

1-((4′-*tert*-Butylbiphenyl-4-yl)ethynyl)-3-ethynylbicyclo-[1.1.1]pentane (10). To a stirred solution of **9** (580 mg, 1.462 mmol) in wet THF (25 mL) was added a solution of TBAF in THF (1.0 M, 2.00 mL, 2.000 mmol) at room temperature. The reddish reaction mixture was stirred for 30 min. The mixture was then diluted with ether (50 mL) and washed with water (2 × 20 mL), and the clear yellowish organic phase was dried over $MgSO_4$. Solvents were removed under reduced pressure, and column chromatography on silica gel (hexane/CH_2Cl_2 = 4:1) gave **10** as a white crystalline solid (465 mg, 1.433 mmol, 98%).

Mp 216.8−218.1 °C. ^{1}H NMR (500 MHz, $CDCl_3$): δ 1.36 (s, 9H), 2.11 (s, 1H), 2.42 (s, 6H), 7.44−7.47 (m, 4H), 7.51−7.54 (m, 4H). ^{13}C NMR (125 MHz, $CDCl_3$): δ 29.9, 30.7, 31.3, 34.6, 58.7, 68.2, 79.9, 82.6, 88.5, 121.3, 125.8, 126.6, 126.7, 132.1, 137.3, 140.7, 150.7. IR (KBr): 3280, 3083, 3032, 2963, 2914, 2877, 2219, 2108, 1611, 1507, 1493, 1478, 1463, 1448, 1394, 1364, 1345, 1268, 1251, 1202, 1113, 1029, 1014, 1003, 966, 950, 924, 852, 821, 764, 748, 742, 724, 687, 658, 645, 572, 546, 532, 507 cm^{-1}. MS m/z (%): 347.2 (100, M + Na), 325.2 (47, M + H). HRMS (ESI+) for ($C_{25}H_{24}$ + H^+): calcd 325.19508, found 325.19504. Anal. Calcd for $C_{25}H_{24}$: C, 92.54; H, 7.46. Found: C, 92.27; H, 7.50.

9,10-Diethynyltriptycene (12).[33] To an ice-cold and well stirred solution of **14** (7.589 g, 16.988 mmol) in wet THF (40 mL) was slowly dropwise added a solution of TBAF in THF (1.0 M, 35.68 mL, 35.675 mmol). The brownish-red reaction mixture was stirred at room temperature for 30 min, diluted with ether (200 mL), and washed with water (3 × 40 mL), and the organic phase was dried over $MgSO_4$. Solvents were removed under reduced pressure, and column chromatography on silica gel (hexane/CH_2Cl_2 = 4:1) afforded **12** as a white crystalline solid (5.066 g, 16.754 mmol, 99%).

^{1}H NMR (400 MHz, $CDCl_3$): δ 3.33 (s, 2H), 7.13−7.15 (m, 6H), 7.79−7.81 (m, 6H). ^{13}C NMR (100 MHz, $CDCl_3$): δ 52.2, 78.0, 80.9, 122.2, 125.8, 142.9, which is in agreement with the literature.[33]

9,10-Bis(trimethylsilylethynyl)anthracene (13).[32] A previously published procedure[32] was adapted as follows: A flame-dried and argon-filled apparatus consisting of a 500 mL two-necked flask equipped with a gas condenser and a magnetic stirrer was charged with 9,10-dibromoanthracene (**11**) (30.000 g, 89.280 mmol), $PdCl_2(PPh_3)_2$ (2.507 g, 3.571 mmol, 4 mol %), and CuI (1.020 g, 5.357 mmol, 6 mol %). After five successive vacuum/argon cycles, dry and degassed Et_2NH (400 mL) was cannulated to the reaction mixture. Finally, TMSA (37.9 mL, 267.840 mmol) was added via syringe. The reaction mixture turned black immediately. The dark solution was refluxed for 6 h and then stirred for 16 h at 70 °C. A dense, dark solid precipitated. All volatiles were removed under reduced pressure, and the black solid residue was suspended in ether (1 L). The dark organic phase was extracted with saturated aq NH_4Cl (3 × 300 mL) and combined aq phases were extracted with ether (3 × 200 mL). Combined ethereal phases were dried over $MgSO_4$, and volatiles were removed under reduced pressure. Column chromatography on silica gel (hexane) gave **13** as a yellow crystalline solid (31.590 g, 85.233 mmol, 95%).

^{1}H NMR (400 MHz, $CDCl_3$): δ 0.46 (s, 18H), 7.62−7.64 (m, 4H), 8.59−8.62 (m, 4H). ^{13}C NMR (100 MHz, $CDCl_3$): δ 0.2, 101.5, 108.1, 118.4, 126.8, 127.2, 132.2, which is in agreement with the literature.[32]

9,10-Bis(trimethylsilylethynyl)triptycene (14).[33] A previously published procedure[33] was adapted as follows: A solution of **13** (31.590 g, 85.233 mmol) in anhydrous DME (400 mL) was canulated to a flame-dried and argon-filled 1 L three-necked flask equipped with a gas condenser, stirrer, and two 250 mL dropping funnels. Isoamyl nitrite (92.8 mL, 690.712 mmol) was dissolved in DME (100 mL) and placed into the first dropping funnel. The second dropping funnel was filled with a solution of anthranilic acid (71.043 g, 518.034 mmol) in DME (150 mL). The solution in the reaction flask was magnetically stirred and heated to gentle reflux (~100 °C) using a heating mantle with a magnetic stirrer. The two solutions in the funnels were slowly dropped into the reaction vessel at the same rate over 6 h. The addition of the solutions was accompanied by rapid evolution of gases

DOI: 10.1021/acs.joc.5b00661
J. Org. Chem. 2015, 80, 6173−6192

(CO_2 and N_2). The reaction mixture turned black and was refluxed for an additional 20 h. All volatiles were removed under reduced pressure and a dark honey-like residue was triturated with boiling hexane (8 × 250 mL). Hexane was evaporated, and the remaining high boiling species were removed under reduced pressure (150 °C, 500 mTorr). (Note: It is crucial to remove all volatiles, mostly isoamyl nitrite and its decomposition products, to ensure sufficient separation during the subsequent column chromatography.) A black solid residue was sorbed on silica gel (20 g) and placed on a column filled with silica gel (500 g). Slow elution (hexane) provided **14** as a white or a slightly yellowish solid (8.638 g, 19.336 mmol, 23%).

^{1}H NMR (400 MHz, $CDCl_3$): δ 0.47 (s, 18H), 7.09−7.11 (m, 6H), 7.70−7.73 (m, 6H). ^{13}C NMR (100 MHz, $CDCl_3$): δ 0.6, 53.2, 98.3, 99.8, 122.4, 125.9, 143.6, which is in agreement with the literature.[33]

9,10-Bis(3-hydroxyprop-1-ynyl)triptycene (15). To a solution of **12** (4.700 g, 15.544 mmol) in THF (200 mL) at −78 °C was dropwise added *n*-BuLi in hexane (2.5 M, 24.87 mL, 62.175 mmol). A dense white precipitate was formed immediately. The white suspension was stirred for 20 min at −78 °C, 30 min at room temperature, and then cooled back to −78 °C. Subsequently, dry solid paraformaldehyde (2.801 g, 93.264 mmol) was added. Cooling was stopped, and the reaction mixture was slowly warmed to room temperature and stirred for 16 h. The suspension turned gray. The reaction was quenched with saturated aq NH_4Cl (40 mL), and the solution was stirred for an additional 60 min. The reaction mixture was diluted with diethyl ether (250 mL) and washed with saturated aq NH_4Cl (4 × 40 mL), and the clear yellow organic phase was dried over $MgSO_4$. Volatiles were removed under reduced pressure. Column chromatography on silica gel (hexane/acetone = 4:3) provided **15** (4.621 g, 12.750 mmol, 82%) as a white crystalline solid.

Mp >310 °C (dec.). ^{1}H NMR (400 MHz, $CDCl_3$): δ 4.82 (s, 4H), 7.08−7.11 (m, 6H), 7.71−7.73 (m, 6H). ^{1}H NMR (400 MHz, acetone-d_6): δ 4.73−4.80 (m, 6H), 7.12−7.15 (m, 6H), 7.77−7.80 (m, 6H). ^{13}C NMR (100 MHz, acetone-d_6): δ 51.0, 53.1, 78.3, 94.3, 123.0, 126.6, 144.6. IR (KBr): 3550, 3403, 3306, 3068, 3059, 3034, 3002, 2938, 2917, 2867, 2254, 1704, 1605, 1460, 1455, 1446, 1391, 1373, 1348, 1309, 1241, 1224, 1215, 1163, 1151, 1133, 1077, 1031, 1018, 1012, 985, 970, 945, 922, 890, 859, 771, 766, 757, 752, 714, 692, 673, 639, 590, 572, 550, 493, 488, 483 cm^{-1}. MS *m*/*z*: 385.2 (M + Na$^+$). HRMS (ESI+) for ($C_{26}H_{18}O_2$ + Na$^+$): calcd 385.11990, found 385.11989. Anal. Calcd for $C_{26}H_{18}O_2$: C, 86.16; H, 5.01. Found: C, 86.31; H, 5.16.

9,10-Bis(3-oxoprop-1-ynyl)triptycene (16). To a solution/suspension of **15** (4.600 g, 12.692 mmol) in dry CH_2Cl_2 (150 mL) was added Dess−Martin periodinane (DMP, 13.458 g, 31.730 mmol) at room temperature. The solution turned yellow immediately, and the reaction mixture was stirred for 2.5 h. The suspension dissolved, leaving a clear yellowish solution. Subsequently, solutions of saturated aq $Na_2S_2O_3$ (50 mL) and $NaHCO_3$ (50 mL) were added, and the mixture was stirred for an additional 15 min. The aqueous phase was removed, and the clear yellowish organic phase was washed with a saturated aqueous solution of $Na_2S_2O_3$ and $NaHCO_3$ in a 1:1 ratio (2 × 50 mL) and finally dried over $MgSO_4$. The solvent was removed under reduced pressure, and a solid yellow residue was sorbed on silica gel (6 g). Column chromatography on silica gel (CH_2Cl_2) afforded **16** as a white crystalline solid (3.257 g, 9.088 mmol, 72%).

Mp >335 °C (dec.). ^{1}H NMR (400 MHz, $CDCl_3$): δ 7.16−7.18 (m, 6H), 7.71−7.73 (m, 6H), 9.74 (s, 2H). ^{13}C NMR (100 MHz, $CDCl_3$): δ 52.4, 89.5, 91.6, 122.2, 126.4, 141.6, 176.1. IR (KBr): 3061, 3034, 3005, 2875, 2230, 2196, 1674, 1608, 1458, 1443, 1385, 1309, 1235, 1179, 1163, 1154, 1074, 1032, 945, 858, 760, 753, 725, 685, 648, 638 cm^{-1}. MS *m*/*z* (%): 358.1 (68, M), 329.1 (62), 313.1 (11), 300.1 (100), 274.1 (23), 224.1 (12), 150.0 (13), 84.0 (8). HRMS (EI) for ($C_{26}H_{14}O_2^+$): calcd 358.0994, found 358.0989. Anal. Calcd for $C_{26}H_{14}O_2$: C, 87.13; H, 3.94. Found: C, 87.13; H, 3.91.

9,10-Bis(4,4-dibromobut-3-en-1-ynyl)triptycene (17). A flame-dried and argon-filled Schlenk flask was charged with PPh_3 (15.223 g, 58.039 mmol) and CBr_4 (8.883 g, 26.787 mmol). After three successive vacuum/argon cycles, the mixture was cooled to 0 °C using an ice bath, dry and degassed CH_2Cl_2 was added (30 mL), and the orange reaction mixture was stirred for 30 min at 0 °C and then for 30 min at room temperature. The solution was cooled back to 0 °C, and a solution of **16** (3.200 g, 8.929 mmol) in dry CH_2Cl_2 (70 mL) was added dropwise. The reaction mixture turned brown immediately. Cooling was stopped, and the brown solution was stirred for an additional 3 h at room temperature. Silica gel (25 g) was added directly to the reaction mixture, and all volatiles were removed under reduced pressure. Column chromatography on silica gel (hexane/CH_2Cl_2 = 1:1) yielded **17** as a white crystalline solid (3.442 g, 5.137 mmol, 58%).

Mp >320 °C (dec.). ^{1}H NMR (400 MHz, $CDCl_3$): δ 7.09 (s, 2H), 7.10−7.13 (m, 6H), 7.75−7.77 (m, 6H). ^{13}C NMR (100 MHz, $CDCl_3$): δ 53.3, 89.4, 91.7, 103.6, 119.3, 122.4, 125.9, 142.9. IR (KBr): 3069, 3059, 3033, 3017, 2222, 1674, 1650, 1604, 1580, 1456, 1313, 1265, 1247, 1162, 1033, 979, 949, 944, 874, 833, 828, 755, 749, 679, 662, 639, 584, 555 cm^{-1}. MS *m*/*z* (%): 669.8 (38, M, center of isotope cluster), 590.9 (12, center of isotope cluster), 509.9 (39, center of isotope cluster), 485.9 (35, center of isotope cluster), 459.9 (30, center of isotope cluster), 430.0 (11, center of isotope cluster), 406.0 (10, center of isotope cluster), 348.1 (78, center of isotope cluster), 324.1 (100, center of isotope cluster), 300.1 (49), 272.1 (17), 248.1 (20), 174.0 (21), 162.0 (26), 149.0 (10), 137.0 (7), 84.0 (12). HRMS (EI) for ($C_{28}H_{14}Br_4^+$): calcd 665.7829, found 665.7826. Anal. Calcd for $C_{28}H_{14}Br_4$: C, 50.19; H, 2.11. Found: C, 50.51; H, 2.16.

9,10-Bis((trimethylsilyl)buta-1,3-diynyl)triptycene (18). The solution of *n*-BuLi in hexane (2.5 M, 9.67 mL, 24.180 mmol) was added dropwise to a solution of **17** (2.700 g, 4.030 mmol) in THF (40 mL) cooled to −78 °C. A dense white precipitate was formed immediately. The suspension was stirred at −78 °C for 90 min, −40 °C for 10 min, and cooled back to −78 °C. Subsequently, TMSCl (4.09 mL, 32.240 mmol) was added, and the solution was stirred at −78 °C for 30 min and finally for 60 min at room temperature. The reaction mixture was diluted with ether (150 mL) and washed with saturated aq NH_4Cl (3 × 30 mL). The clear yellowish organic phase was dried over $MgSO_4$, and volatiles were removed under reduced pressure. Column chromatography on silica gel (hexane/CH_2Cl_2 = 5:1) gave **18** as a white crystalline solid (1.664 g, 3.363 mmol, 90%).

Mp >350 °C (dec.). ^{1}H NMR (400 MHz, $CDCl_3$): δ 0.35 (s, 18H), 7.11−7.13 (m, 6H), 7.72−7.74 (m, 6H). ^{13}C NMR (100 MHz, $CDCl_3$): δ −0.4, 52.8, 72.2, 77.2, 87.4, 87.7, 122.3, 126.0, 142.8. IR (KBr): 3071, 3034, 2956, 2897, 2261, 2230, 2106, 1605, 1462, 1454, 1442, 1411, 1304, 1251, 1172, 1155, 1145, 1099, 1032, 1004, 977, 956, 844, 760, 747, 710, 670 cm^{-1}. MS *m*/*z*: 495.3 (M + H). HRMS (ESI+) for ($C_{34}H_{30}Si_2$ + H$^+$): calcd 495.19588, found 495.19577. Anal. Calcd for $C_{34}H_{30}Si_2$: C, 82.54; H, 6.11. Found: C, 82.32; H, 6.26.

Desymmetrization of Tetrayne 18. To a solution of **18** (1.600 g, 3.234 mmol) in THF (140 mL) cooled to 0−5 °C in an ice bath was slowly added (0.05 mL/min) a solution of MeLi in ether (1.6 M, 2.43 mL, 3.881 mmol). The reaction mixture was stirred at this temperature for an additional 3 h. A dense white solid precipitated. Progress of the reaction was monitored by TLC (hexane/CH_2Cl_2 = 4:1). The solution was diluted with ether (150 mL) and washed with saturated aq NH_4Cl (2 × 30 mL), and the clear yellowish organic phase was dried over $MgSO_4$. Solvents were removed under reduced pressure, and the yellowish solid residue was purified using column chromatography on silica gel (hexane/CH_2Cl_2 = 4:1). Compounds were eluted from the column in the following order: **18** (210 mg, 0.424 mmol, 13%), **19** (654 mg, 1.548 mmol, 48%), and **20** (440 mg, 1.256 mmol, 39%). All three compounds were obtained as white crystalline solids.

9-((Trimethylsilyl)buta-1,3-diynyl)-10-(buta-1,3-diynyl)-triptycene (19). Mp >240 °C (dec.). ^{1}H NMR (400 MHz, $CDCl_3$): δ 0.35 (s, 9H), 2.43 (s, 1H), 7.12−7.14 (m, 6H), 7.71−7.75 (m, 6H). ^{13}C NMR (100 MHz, $CDCl_3$): δ −0.4, 52.6, 52.8, 67.7, 68.6, 71.2, 72.2, 76.5, 77.3, 87.4, 87.8, 122.2, 122.4, 126.0, 126.1, 142.6, 142.8. IR (KBr): 3303, 3071, 3034, 2957, 2928, 2254, 2252, 2112, 2119, 1605, 1453, 1442, 1422, 1411, 1304, 1251, 1170, 1153, 1088, 1032, 1008, 950, 906, 880, 843, 750, 735, 705, 639 cm^{-1}. MS *m*/*z* (%): 445.2 (100, M + Na$^+$), 423.2 (18, M + H$^+$). HRMS (ESI+) for ($C_{31}H_{22}Si$ + Na$^+$): calcd 445.13830, found 445.13824. Anal. Calcd for $C_{31}H_{22}Si$: C, 88.11; H, 5.25. Found: C, 88.27; H, 5.12.

DOI: 10.1021/acs.joc.5b00661
J. Org. Chem. 2015, 80, 6173−6192

9,10-Di(buta-1,3-diynyl)triptycene (20). Mp >190 °C (dec.). ^{1}H NMR (400 MHz, $CDCl_3$): δ 2.44 (s, 2H), 7.13−7.15 (m, 6H), 7.72−7.75 (m, 6H). ^{13}C NMR (100 MHz, $CDCl_3$): δ 52.6, 67.6, 68.6, 71.1, 76.5, 122.3, 126.1, 142.6. IR (KBr): 3285, 3270, 3069, 3060, 3048, 3034, 3020, 3004, 2246, 2217, 2109, 1606, 1581, 1456, 1443, 1311, 1262, 1247, 1168, 1161, 1151, 1144, 1032, 984, 975, 947, 940, 922, 907, 876, 867, 859, 755, 749, 701, 650, 638 cm^{-1}. MS m/z (%): 351.1 (100, M + H). HRMS (APCI) for ($C_{28}H_{14}$ + H^+): calcd 351.11683, found 351.11642. Anal. Calcd for $C_{28}H_{14}$: C, 95.97; H, 4.03. Found: C, 95.60; H, 3.93.

1-(2,2-Dibromoethyl)-3,5,7-trimethyladamantane (22).[34] A previously published procedure[34] was adapted as follows. A flame-dried and argon-filled apparatus consisting of a 50 mL three-necked flask equipped with a stirrer, septa, L-shaped glass tubing for the addition of solids, and a connector to the vacuum/argon line was charged with 1-bromo-3,5,7-trimethyladamantane (**21**) (1.500 g, 5.832 mmol), and the L-shaped tubing was charged with anhydrous powdered $AlBr_3$ (621 mg, 2.334 mmol). After three successive vacuum/argon cycles, an anhydrous vinyl bromide (6.00 mL, 85.554 mmol) was added at −78 °C. Subsequently, the $AlBr_3$ from the L-shaped tubing was added to the reaction mixture, and the solution was vigorously stirred at −78 °C for 3 h. A dense white solid precipitated. The well-stirred reaction mixture was quenched by the dropwise addition of water (5 mL). Cooling was stopped, and the reaction mixture was heated to room temperature, allowing spontaneous evaporation of vinyl bromide. An additional portion of water (10 mL) was added; the suspension was extracted with ether (3 × 25 mL), and the combined ethereal phases were dried over $MgSO_4$. The colorless ethereal phase was concentrated, and the yellowish oily residue was distilled using a Kugelrohr distillation apparatus (600 mTorr, 180 °C). Product **22** was obtained as a clear colorless liquid (1.593 g, 4.374 mmol, 75%).

^{1}H NMR (400 MHz, $CDCl_3$): δ 0.82 (s, 9H), 1.04 (s, 6H), 1.18 (s, 6H), 2.57 (d, J = 6.05 Hz, 2H), 5.82 (t, J = 6.05 Hz, 1H). ^{13}C NMR (100 MHz, $CDCl_3$): δ 30.2, 31.9, 37.2, 40.1, 47.7, 50.2, 59.3. IR (KBr): 2945, 2919, 2894, 2862, 2835, 1454, 1429, 1374, 1355, 1254, 1247, 1225, 1165, 1144, 1028, 936, 915, 872, 799, 691, 585, 562, 439 cm^{-1}. MS m/z (%): 363.0 (2, M), 177.2 (100, M − CH_2CHBr_2). HRMS (CI) for ($C_{15}H_{23}Br_2^+$): calcd 361.0166, found 361.0172. Anal. Calcd for $C_{15}H_{24}Br_2$: C, 49.47; H, 6.64. Found: C, 49.24; H, 6.56, which is in agreement with the literature.[34]

1-Ethynyl-3,5,7-trimethyladamantane (23).[34] A flame-dried Schlenk flask was charged with *t*-BuOK (1.294 g, 11.532 mmol). After three successive vacuum/argon cycles, THF (5 mL) was added from a syringe. Subsequently, a solution of **22** (1.400 g, 3.844 mmol) in THF (10 mL) was added dropwise at 0 °C. Cooling was stopped, and the reaction mixture was stirred at room temperature for 3 d. A dense, white solid precipitated. The crude reaction mixture was diluted with ether (80 mL), and water (10 mL) was slowly added. The slightly yellowish organic phase was washed with water (2 × 20 mL) and saturated aq NH_4Cl (1 × 20 mL) and dried over $MgSO_4$. Solvents were removed under reduced pressure, and the yellowish solid residue was purified using column chromatography on silica gel (hexane) to give **23** (663 mg, 3.277 mmol, 85%) as a colorless liquid, which solidified in the refrigerator.

^{1}H NMR (400 MHz, $CDCl_3$): δ 0.83 (s, 9H), 1.01−1.04 (m, 3H), 1.08−1.11 (m, 3H), 1.44 (s, 6H), 2.08 (s, 1H). ^{13}C NMR (100 MHz, $CDCl_3$): δ 29.9, 31.60, 31.63, 48.2, 49.8, 66.7, 92.3. IR (KBr): 3312, 2947, 2894, 2864, 2837, 2106, 1454, 1375, 1354, 1255, 1231, 912, 627, 553, 529 cm^{-1}. MS m/z (%): 203.2 (100, M + H), 187.1 (65), 177.2 (14), 161.1 (8), 147.1 (13), 133.1 (5), 121.1 (12). HRMS (CI) for ($C_{15}H_{22}$ + H^+): calcd 203.1800, found 203.1796. Anal. Calcd for $C_{15}H_{22}$: C, 89.04; H, 10.96. Found: C, 88.98; H, 10.96, which is in agreement with the literature.[34]

1-(2,3-Dichloro-4-iodophenyl)ethynyl-3,5,7-trimethyladamantane (25). A flame-dried Schlenk flask was charged with **23** (200 mg, 0.988 mmol), 1,4-diiodo-2,3-dichlorobenzene (**24**) (1.970 g, 4.940 mmol, 5 equiv), $Pd(PPh_3)_4$ (46 mg; 0.040 mmol, 4 mol %), and CuI (6 mg, 0.030 mmol, 3 mol %). After three successive vacuum/argon cycles, dry and degassed THF (5 mL) and triethylamine (10 mL) were added from a syringe. The slightly yellowish solution was stirred for 5 h at 40 °C. A dense white solid precipitated. The crude reaction mixture was diluted with ether (80 mL) and washed with saturated aq NH_4Cl (2 × 30 mL). The clear yellowish organic phase was dried over $MgSO_4$, and volatiles were removed under reduced pressure. Column chromatography repeated four times on silica gel (hexane) provided **25** as a colorless viscous oil (394 mg, 0.833 mmol, 84%).

^{1}H NMR (400 MHz, $CDCl_3$): δ 0.86 (s, 9H), 1.04−1.07 (m, 3H), 1.12−1.15 (m, 3H), 1.53 (s, 6H), 7.00 (d, J = 8.29 Hz, 1H), 7.66 (d, J = 8.29 Hz, 1H). ^{13}C NMR (100 MHz, $CDCl_3$): δ 29.9, 31.7, 32.8, 47.8, 49.9, 76.1, 97.4, 105.3, 126.0, 131.6, 134.1, 137.1, 137.4. IR (KBr): 2944, 2917, 2891, 2861, 2838, 2230, 1452, 1436, 1414, 1374, 1351, 1285, 1253, 1226, 1167, 1139, 1076, 927, 873, 829, 814, 783, 760, 621, 578, 524 cm^{-1}. MS m/z (%): 472.0 (82, M, center of isotope cluster), 457.0 (16, M − CH_3, center of isotope cluster), 374.2 (25, center of isotope cluster), 346.1 (71, M − I), 177.2 (100, 3,5,7-trimethyladamantyl). HRMS (CI) for ($C_{21}H_{23}Cl_2I^+$): calcd 472.0222, found 472.0211. Anal. Calcd for $C_{21}H_{23}Cl_2I$: C, 53.30; H, 4.90. Found: C, 53.37; H, 4.84.

Bis((3,5,7-trimethyladamantyl)-1-ethynyl)-2,3-dichlorobenzene (26). The title compound was isolated as a more polar side-product during the chromatography described above as a white crystalline solid (33 mg, 0.060 mmol, 12%).

Mp 226.3−227.9 °C. ^{1}H NMR (400 MHz, $CDCl_3$): δ 0.86 (s, 18H), 1.04−1.07 (m, 6H), 1.12−1.15 (m, 6H), 1.53 (s, 12H), 7.20 (s, 2H). ^{13}C NMR (100 MHz, $CDCl_3$): δ 30.0, 31.7, 32.8, 47.9, 49.9, 76.5, 105.1, 124.6, 130.2, 134.6. IR (KBr): 2948, 2916, 2863, 2841, 2229, 1454, 1374, 1363, 1350, 1287, 1253, 1226, 1214, 1065, 1054, 938, 920, 910, 884, 830, 807, 774, 686, 612, 569, 551, 528, 511 cm^{-1}. MS m/z (%): 547.3 (100, M + H). HRMS (APCI) for ($C_{36}H_{44}Cl_2$ + H^+): calcd 547.28928, found 547.28927. Anal. Calcd for $C_{36}H_{44}Cl_2$: C, 78.95; H, 8.10. Found: C, 78.62; H, 8.06.

9-((2,3-Dichlorophenyl)buta-1,3-diynyl)-10-((trimethylsilyl)-buta-1,3-diynyl)triptycene (28). A flame-dried Schlenk flask was charged with **19** (260 mg, 0.615 mmol), 1,2-dichloro-3-iodobenzene (**27**) (201 mg, 0.738 mmol), $Pd(PPh_3)_4$ (29 mg, 0.025 mmol, 4 mol %) and CuI (3 mg, 0.018 mmol, 3 mol %). After three successive vacuum/argon cycles, degassed dry THF (8 mL) and triethylamine (5 mL) were added from a syringe. The yellow solution was stirred for 18 h at room temperature. A dense white solid precipitated. The crude reaction mixture was diluted with CH_2Cl_2 (150 mL) and washed with saturated aq NH_4Cl (2 × 30 mL), and the yellow organic phase was dried over $MgSO_4$. Column chromatography on silica gel (hexane/CH_2Cl_2 = 4:1) gave **28** as a white crystalline solid (236 mg, 0.416 mmol, 68%).

Mp >300 °C (dec.). ^{1}H NMR (400 MHz, $CDCl_3$): δ 0.36 (s, 9H), 7.13−7.15 (m, 6H), 7.23 (t, J = 7.93 Hz, 1H), 7.52 (dd, J_1 = 1.30 Hz, J_2 = 8.08 Hz, 1H), 7.62 (dd, J_1 = 1.33 Hz, J_2 = 7.73 Hz, 1H), 7.74−7.79 (m, 6H). ^{13}C NMR (100 MHz, $CDCl_3$): δ −0.4, 52.8, 53.1, 72.2, 74.4, 76.5, 77.3, 78.9, 79.4, 87.4, 87.8, 122.3, 122.4, 123.8, 126.0, 126.1, 127.2, 131.3, 132.7, 133.6, 135.5, 142.7, 142.8. IR (KBr): 3069, 3033, 3015, 3007, 2111, 1606, 1577, 1550, 1453, 1409, 1341, 1304, 1251, 1192, 1166, 1152, 1110, 1050, 1032, 970, 948, 939, 922, 860, 843, 784, 750, 744, 707, 639 cm^{-1}. MS m/z (%): 567.1 (100, M + H, center of isotope cluster), 495.1 (43, M − TMS, center of isotope cluster). HRMS (APCI) for ($C_{37}H_{24}Cl_2Si$ + H^+): calcd 567.10971, found 567.10931. Anal. Calcd for $C_{37}H_{24}Cl_2Si$: C, 78.30; H, 4.26. Found: C, 78.67; H, 4.47.

Compound 29. A flame-dried Schlenk flask was charged with **25** (200 mg, 0.423 mmol), **19** (197 mg, 0.465 mmol), $Pd(PPh_3)_4$ (20 mg; 0.017 mmol, 4 mol %), and CuI (2 mg, 0.013 mmol, 3 mol %). After three successive vacuum/argon cycles, degassed dry THF (6 mL) and triethylamine (6 mL) were added from a syringe. The yellow solution was stirred for 18 h at room temperature. A dense white solid precipitated. The crude reaction mixture was diluted with ether (80 mL) and washed with saturated aq NH_4Cl (2 × 30 mL), and the yellowish organic phase was dried over $MgSO_4$. Volatiles were removed under reduced pressure. Column chromatography on silica gel (hexane/CH_2Cl_2 = 6:1) gave **29** as a white foamy solid (238 mg, 0.310 mmol, 73%).

DOI: 10.1021/acs.joc.5b00661
J. Org. Chem. 2015, 80, 6173−6192

Mp 172.3−174.3 °C. ^{1}H NMR (400 MHz, $CDCl_3$): δ 0.35 (s, 9H), 0.89 (s, 9H), 1.08−1.11 (m, 3H), 1.16−1.19 (m, 3H), 1.57 (s, 6H), 7.13−7.15 (m, 6H), 7.34 (d, J = 8.13 Hz, 1H), 7.51 (d, J = 8.12 Hz, 1H), 7.74−7.77 (m, 6H). ^{13}C NMR (100 MHz, $CDCl_3$): δ −0.3, 30.0, 31.7, 32.9, 47.8, 49.9, 52.8, 53.1, 72.2, 74.7, 76.49, 76.53, 77.3, 79.7, 79.9, 87.4, 87.7, 107.1, 122.1, 122.3, 122.4, 126.0, 126.1, 126.9, 130.6, 131.6, 135.2, 135.9, 142.7, 142.8. IR (KBr): 3069, 3034, 2945, 2916, 2891, 2862, 2836, 2225, 2109, 1607, 1579, 1453, 1366, 1353, 1252, 1227, 1211, 1150, 1141, 1084, 1032, 941, 910, 845, 790, 752, 712, 677, 639, 608, 560, 550, 525, 500, 478 cm^{-1}. MS m/z (%): 767.3 (100, M + H). HRMS (APCI) for ($C_{52}H_{44}Cl_2Si$ + H^+): calcd 767.26621, found 767.26642. Anal. Calcd for $C_{52}H_{44}Cl_2Si$: C, 81.33; H, 5.78. Found: C, 81.12; H, 5.86.

9-Trimethylsilylethynyl-10-ethynyltriptycene (30). To a solution of **14** (5.530 g, 12.379 mmol) in THF (120 mL) cooled to 0−5 °C in an ice bath was slowly (0.05 mL/min) added a solution of MeLi in ether (1.6 M, 10.06 mL, 16.093 mmol). The reaction mixture was stirred at this temperature for additional 60 min, during which time a dense white precipitate was formed. Progress of the reaction was monitored by TLC (hexane/CH_2Cl_2 = 4:1). The solution was diluted with ether (150 mL) and washed with saturated aq NH_4Cl (2 × 30 mL), and the clear yellowish organic phase was dried over $MgSO_4$. Solvents were removed under reduced pressure, and the yellowish solid residue was purified using column chromatography on silica gel (hexane/CH_2Cl_2 = 4:1). Compounds were eluted from the column in following order: **14** (542 mg, 1.213 mmol, 10%), **30** (2.662 g, 7.107 mmol, 57%) and **12** (1.175 g, 3.886 mmol, 31%). All three compounds were obtained as white crystalline solids.

Mp 213.0−214.2 °C. ^{1}H NMR (400 MHz, $CDCl_3$): δ 0.47 (s, 9H), 3.30 (s, 1H), 7.10−7.12 (m, 6H), 7.72−7.76 (m, 6H). ^{13}C NMR (100 MHz, $CDCl_3$): δ 0.3, 52.1, 53.0, 78.1, 80.9, 98.2, 99.4, 122.1, 122.3, 125.7, 125.8, 143.0, 143.2. IR (KBr): 3288, 3068, 3034, 3016, 2958, 2898, 2181, 2149, 2129, 1622, 1608, 1457, 1454, 1448, 1427, 1418, 1409, 1330, 1302, 1252, 1221, 1168, 1158, 1075, 1037, 1032, 1007, 981, 950, 857, 842, 753, 701, 692, 666, 648, 640, 614 cm^{-1}. MS m/z (%): 375.2 (100, M + H). HRMS (APCI) for ($C_{27}H_{22}Si$ + H^+): calcd 375.15635, found 375.15651. Anal. Calcd for $C_{27}H_{22}Si$: C, 86.58; H, 5.92. Found: C, 86.41; H, 5.90.

9-Bromoethynyl-10-(trimethylsilylethynyl)triptycene (31). Freshly recrystallized NBS (63 mg, 0.353 mmol) and $AgNO_3$ (12 mg, 0.074 mmol) were added to a solution of **30** (110 mg, 0.294 mmol) in dry acetone (10 mL) at 25 °C. The slightly yellowish solution was stirred at room temperature in the dark for 2.5 h. A white solid precipitated. Solvent was removed under reduced pressure, and column chromatography on silica gel (hexane/CH_2Cl_2 = 4:1) gave **31** as a white crystalline solid (111 mg, 0.245 mmol, 83%).

Mp 247.7−248.9 °C. ^{1}H NMR (500 MHz, $CDCl_3$): δ 0.47 (s, 9H), 7.11−7.12 (m, 6H), 7.69−7.74 (m, 6H). ^{13}C NMR (125 MHz, $CDCl_3$): δ 0.3, 51.4, 52.9, 53.3, 74.8, 98.2, 99.3, 122.1, 122.3, 125.7, 125.8, 143.1. IR (KBr): 3070, 3034, 3018, 2959, 2897, 2217, 2173, 1608, 1453, 1422, 1409, 1328, 1303, 1262, 1250, 1226, 1168, 1158, 1140, 1090, 1048, 1032, 976, 949, 857, 843, 752, 711, 698, 645, 640, 488 cm^{-1}. MS m/z (%): 477.10 (100, M + H, center of isotope cluster). HRMS (ESI+) for ($C_{27}H_{21}BrSi$ + Na^+): calcd 475.04881, found 475.04866. Anal. Calcd for $C_{27}H_{21}BrSi$: C, 71.52; H, 4.67. Found: C, 71.42; H, 4.53.

3-(3-((4′-*tert*-Butylbiphenyl-4-yl)ethynyl)bicyclo[1.1.1]pent-1-yl)propiolaldehyde (32). To a solution of DMSO (140 μL, 1.974 mmol) in CH_2Cl_2 (5 mL) was added $(COCl)_2$ (119 μL, 1.410 mmol) at −78 °C. After 30 min at this temperature, **33** (100 mg, 0.282 mmol) in CH_2Cl_2 (25 mL) was slowly introduced, and the milky solution was stirred 90 min at −78 °C. Then, triethylamine (393 μL, 2.820 mmol) was added, and the reaction mixture was stirred for 60 min and warmed to room temperature. A white precipitate dissolved, leaving a clear yellow solution. Volatiles were removed under reduced pressure, and the yellowish solid residue was sorbed on silica gel (4 g). Column chromatography on silica gel (hexane/CH_2Cl_2 = 1:1) yielded **32** as a white crystalline solid (81 mg, 0.230 mmol, 82%).

Mp 237−239 °C (dec.). ^{1}H NMR (400 MHz, $CDCl_3$): δ 1.36 (s, 9H), 2.51 (s, 6H), 7.44−7.48 (s, 4H), 7.52−7.54 (s, 4H), 9.19 (s, 1H). ^{13}C NMR (100 MHz, $CDCl_3$): δ 29.6, 31.3, 31.7, 34.6, 58.9, 79.8, 80.6, 87.7, 94.8, 121.0, 125.8, 126.6, 126.7, 132.1, 137.3, 140.9, 150.8, 176.7. IR (KBr): 3032, 2991, 2954, 2944, 2914, 2900, 2876, 2225, 2197, 1663, 1492, 1462, 1393, 1376, 1367, 1358, 1271, 1201, 1109, 1004, 951, 907, 852, 837, 821, 749, 725, 671, 573, 547, 532 cm^{-1}. MS m/z (%): 375.2 (100, M + Na). HRMS (ESI+) for ($C_{26}H_{24}O$ + Na^+): calcd 375.17194, found 375.17184. Anal. Calcd for $C_{26}H_{24}O$: C, 88.60; H, 6.86. Found: C, 88.23; H, 6.87.

3-(3-((4′-*tert*-Butylbiphenyl-4-yl)ethynyl)bicyclo[1.1.1]pent-1-yl)prop-2-yn-1-ol (33). To a solution of **10** (140 mg, 0.431 mmol) in ether (8 mL) was added *n*-BuLi in hexane (2.5 M, 520 μL, 1.300 mmol) dropwise at −78 °C. A dense white precipitate was formed immediately. The slightly yellowish solution was stirred at −78 °C for 5 min, heated to room temperature, and then cooled back to −78 °C. Subsequently, dry paraformaldehyde (66 mg, 2.200 mmol) was added, and the white suspension was stirred for an additional 60 min at −78 °C. Cooling was stopped, and the reaction mixture was slowly warmed to room temperature and stirred for an additional 16 h. The suspension turned yellow. The reaction was quenched with saturated aq NH_4Cl (10 mL), and the solution was stirred for an additional 20 min. The reaction mixture was diluted with ether (80 mL) and washed with saturated aq NH_4Cl (2 × 20 mL). Combined water phases were extracted with ether (1 × 30 mL). The clear yellow organic phase was dried over $MgSO_4$, and volatiles were removed under reduced pressure. Column chromatography on silica gel (CH_2Cl_2) gave **33** as a white crystalline solid (117 mg, 0.330 mmol, 77%).

Mp 258−264 °C (dec.). ^{1}H NMR (400 MHz, $CDCl_3$): δ 1.35 (s, 9H), 1.54 (br s, 1H), 2.40 (s, 6H), 4.27 (s, 2H), 7.43−7.47 (m, 4H), 7.51−7.53 (m, 4H). ^{13}C NMR (100 MHz, $CDCl_3$): δ 30.1, 30.8, 31.3, 34.6, 51.3, 58.7, 78.2, 80.0, 84.6, 88.5, 121.4, 125.8, 126.6, 126.7, 132.1, 137.3, 140.6, 150.7. IR (KBr): 3334, 3083, 3028, 2994, 2961, 2914, 2877, 1492, 1462, 1447, 1394, 1359, 1275, 1201, 1108, 1020, 1003, 937, 897, 857, 843, 822, 749, 742, 725, 574, 546 cm^{-1}. MS m/z (%): 377.0 (100, M + Na). HRMS (ESI+) for ($C_{26}H_{26}O$ + Na^+): calcd 377.18759, found 377.18768. Anal. Calcd for $C_{26}H_{26}O$: C, 88.09; H, 7.39. Found: C, 88.39; H, 7.24.

3-(3-((4′-*tert*-Butylbiphenyl-4-yl)ethynyl)bicyclo[1.1.1]pent-1-yl)propiolic Acid (34). A solution of *n*-BuLi in hexane (2.5 M, 148 μL, 0.370 mmol) was added dropwise to a stirred solution of **10** (60 mg, 0.185 mmol) in THF (10 mL) at −78 °C. The slightly yellowish solution was stirred at −78 °C for 15 min, heated to room temperature, and then cooled back to −78 °C. Gaseous CO_2 was bubbled into the solution through a PTFE cannula at −78 °C for 10 min and at room temperature for an additional 10 min. A dense white solid precipitated. The white suspension was diluted with water (10 mL), acidified with concentrated HCl (pH ≈1), and extracted with ether (4 × 30 mL), and the combined colorless ethereal phases were dried over $MgSO_4$. Solvents were removed under reduced pressure, and the white solid residue was triturated with CH_2Cl_2 (3 × 3 mL). Carboxylic acid **34** was obtained as a white crystalline solid (63 mg, 0.171 mmol, 92%).

Mp 265 °C (dec). ^{1}H NMR (400 MHz, THF-d_8): δ 1.33 (s, 9H), 2.43 (s, 6H), 7.40−7.46 (m, 4H), 7.53−7.58 (m, 4H). ^{13}C NMR (100 MHz, THF-d_8): δ 30.3, 31.6, 32.2, 35.2, 59.4, 73.6, 81.0, 84.6, 88.5, 122.4, 126.5, 127.2, 127.3, 132.9, 138.1, 141.7, 151.4, 154.2. IR (KBr): 3434, 3083, 3032, 2993, 2960, 2916, 2902, 2879, 2233, 1686, 1493, 1478, 1462, 1448, 1418, 1394, 1364, 1348, 1293, 1238, 1203, 1180, 1113, 1095, 1029, 1004, 926, 876, 851, 820, 753, 748, 724, 657, 636, 601, 572, 547 cm^{-1}. MS m/z (%): 367.1 (38, M − H), 323.1 (100, M − COOH). HRMS (ESI−) for ($C_{26}H_{23}O_2^-$): calcd 367.17035, found 367.17052. Anal. Calcd for $C_{26}H_{24}O_2$: C, 84.75; H, 6.57. Found: C, 84.64; H, 6.55.

Methyl 3-(3-((4′-*tert*-Butylbiphenyl-4-yl)ethynyl)bicyclo-[1.1.1]pent-1-yl)propiolate (35). An ethereal solution of CH_2N_2 was added dropwise to a solution of **34** (55 mg, 0.149 mmol) in ether (10 mL) at room temperature until the reaction mixture turned yellow. The solution was stirred for 10 min, and volatiles were removed under reduced pressure. Column chromatography on silica gel (hexane/CH_2Cl_2 = 1:1) yielded **35** as a white crystalline solid (53 mg, 0.139 mmol, 93%).

DOI: 10.1021/acs.joc.5b00661
J. Org. Chem. 2015, 80, 6173−6192

Mp 233.4−234.9 °C. ^{1}H NMR (400 MHz, $CDCl_3$): δ 1.36 (s, 9H), 2.48 (s, 6H), 3.77 (s, 3H), 7.43−7.47 (m, 4H), 7.51−7.53 (m, 4H). ^{13}C NMR (100 MHz, $CDCl_3$): δ 29.3, 31.3, 31.4, 34.5, 52.8, 58.8, 71.6, 80.4, 86.1, 87.9, 121.1, 125.8, 126.6, 126.7, 132.1, 137.3, 140.8, 150.7, 153.9. IR (KBr): 3032, 2994, 2960, 2913, 2876, 2233, 1709, 1675, 1610, 1492, 1457, 1438, 1396, 1360, 1289, 1215, 1178, 1113, 1091, 1030, 1003, 979, 865, 856, 822, 753, 725, 678, 573, 545 cm^{-1}. MS m/z (%): 405.2 (100, M + Na). HRMS (ESI+) for ($C_{27}H_{26}O_2$ + Na^+): calcd 405.18250, found 405.18245. Anal. Calcd for $C_{27}H_{26}O_2$: C, 84.78; H, 6.85. Found: C, 84.66; H, 6.90.

Compound 36. To a solution of **30** (127 mg, 0.340 mmol) in THF (2 mL) was dropwise added *n*-BuLi in hexane (2.5 M, 102 μL, 0.255 mmol) at −78 °C. A dense white precipitate was formed immediately. The slightly yellowish suspension was stirred at −78 °C for 15 min, heated to room temperature, and then cooled to −78 °C again. Subsequently, a solution of **32** (60 mg, 0.170 mmol) in THF (6 mL) was added, and the reaction mixture was stirred for 60 min at −78 °C. Cooling was stopped, and the reaction mixture was slowly warmed to room temperature and stirred for 30 min. The suspension dissolved, leaving a clear yellow solution. The reaction mixture was diluted with ether (60 mL) and washed with saturated aq NH_4Cl (2 × 20 mL), and the clear yellow organic phase was dried over $MgSO_4$. Volatiles were removed under reduced pressure, and column chromatography on silica gel (hexane/CH_2Cl_2 = 1:1, then pure CH_2Cl_2) gave racemic **36** as a white crystalline solid (117 mg, 0.161 mmol, 95%).

Mp 164.7−165.9 °C. ^{1}H NMR (400 MHz, $CDCl_3$): δ 0.48 (s, 9H), 1.36 (s, 9H), 2.50 (s, 6H), 5.62 (s, 1H), 7.11−7.13 (m, 6H), 7.46−7.48 (m, 4H), 7.52−7.54 (m, 4H), 7.71−7.75 (m, 6H). ^{13}C NMR (100 MHz, $CDCl_3$): δ 0.3, 30.1, 31.1, 31.3, 34.6, 52.0, 52.8, 53.0, 58.8, 77.6, 79.3, 80.2, 83.9, 88.4, 90.5, 98.2, 99.4, 121.3, 122.1, 122.3, 125.7, 125.78, 125.83, 126.6, 126.7, 132.1, 137.3, 140.7, 143.1, 143.2, 150.7. IR (KBr): 3549, 3293, 3069, 3032, 2962, 2914, 2878, 2245, 2216, 2180, 1608, 1494, 1454, 1446, 1394, 1363, 1309, 1297, 1271, 1251, 1230, 1166, 1155, 1141, 1113, 1055, 1032, 1004, 975, 853, 843, 821, 753, 692, 649, 640, 611, 573, 545, 486 cm^{-1}. MS m/z (%): 749.3 (100, M + Na). HRMS (ESI+) for ($C_{53}H_{46}OSi$ + Na^+): calcd 749.32101, found 749.32071. Anal. Calcd for $C_{53}H_{46}OSi$: C, 87.56; H, 6.38. Found: C, 87.57; H, 6.15.

Compound 37. To a solution of DMSO (137 μL, 1.932 mmol) in CH_2Cl_2 (2 mL) was added $(COCl)_2$ (117 μL, 1.380 mmol) at −78 °C. After 30 min at this temperature, **36** (100 mg, 0.138 mmol) in CH_2Cl_2 (4 mL) was slowly introduced, and the milky solution was stirred for 60 min at −78 °C. Then, triethylamine (385 μL, 2.760 mmol) was added. The mixture was stirred for 10 min, warmed to room temperature, and stirred for an additional 30 min. The solution turned yellow and contained a dense white precipitate. Volatiles were removed under reduced pressure, and the yellowish solid was sorbed on silica gel (4 g). Column chromatography on silica gel (hexane/CH_2Cl_2 = 1:1) afforded **37** as a white crystalline solid (79 mg, 0.109 mmol, 79%).

Mp >245 °C (dec.). ^{1}H NMR (400 MHz, $CDCl_3$): δ 0.49 (s, 9H), 1.37 (s, 9H), 2.61 (s, 6H), 7.14−7.16 (m, 6H), 7.47−7.49 (m, 4H), 7.53−7.56 (m, 4H), 7.69−7.71 (m, 3H), 7.75−7.77 (m, 3H). ^{13}C NMR (100 MHz, $CDCl_3$): δ 0.3, 29.7, 31.3, 31.8, 34.6, 52.2, 53.1, 59.0, 80.7, 80.9, 87.4, 87.8, 92.1, 92.5, 98.5, 99.0, 121.0, 121.9, 122.6, 125.8, 125.9, 126.2, 126.6, 126.7, 132.1, 137.3, 140.9, 142.0, 143.0, 150.8, 160.1. IR (KBr): 3070, 3033, 2993, 2958, 2915, 2878, 2222, 2207, 2178, 1645, 1608, 1507, 1493, 1458, 1454, 1445, 1395, 1362, 1309, 1281, 1261, 1251, 1231, 1183, 1159, 1131, 1113, 1057, 1044, 1032, 1024, 1005, 857, 843, 821, 744, 719, 690, 652, 639, 623, 590, 574, 547, 491, 485 cm^{-1}. MS m/z (%): 725.2 (100, M + H). HRMS (ESI+) for ($C_{53}H_{44}OSi$ + H^+): calcd 725.32342, found 725.32324. Anal. Calcd for $C_{53}H_{44}OSi$: C, 87.80; H, 6.12. Found: C, 87.65; H, 5.95.

1,1,1,3,3,3-Hexamethyl-2-(trimethylsilyl)-2-((4-((trimethylsilyl)ethynyl)phenyl)ethynyl)trisilane (39). A flame-dried Schlenk flask was charged with **40** (776 mg, 2.844 mmol), ((4-bromophenyl)ethynyl)trimethylsilane (**41**) (600 mg, 2.370 mmol), $Pd(PPh_3)_4$ (110 mg, 0.095 mmol, 4 mol %), and CuI (14 mg, 0.071 mmol, 3 mol %). After three successive vacuum/argon cycles, dry and degassed THF (10 mL) and triethylamine (5 mL) were added from a syringe. The yellow solution was stirred for 3 days at 55 °C. A dense white solid precipitated, and the mixture turned black. The crude reaction mixture was diluted with ether (80 mL) and washed with saturated aq NH_4Cl (2 × 30 mL), and a brownish organic phase was dried over $MgSO_4$. Column chromatography on silica gel (hexane) gave **39** as a colorless oil (867 mg, 1.948 mmol, 82%).

^{1}H NMR (400 MHz, $CDCl_3$): δ 0.24 (s, 27H), 0.25 (s, 9H), 7.30−7.37 (m, 4H). ^{13}C NMR (100 MHz, $CDCl_3$): δ −0.05, 0.4, 91.0, 95.8, 104.8, 107.9, 122.2, 124.7, 131.5, 131.7. IR (KBr): 3079, 3037, 2958, 2895, 2828, 2158, 1505, 1494, 1441, 1404, 1246, 1221, 1101, 1018, 866, 836, 788, 759, 747, 691, 645, 623, 550, 434 cm^{-1}. MS m/z (%): 445.2 (82, M + H), 429.2 (100, M - CH_3). HRMS (CI) for ($C_{22}H_{40}Si_5$ + H^+): calcd 445.2055, found 445.2061. Anal. Calcd for $C_{22}H_{40}Si_5$: C, 59.38; H, 9.06. Found: C, 59.46; H, 9.09.

2-Ethynyl-1,1,1,3,3,3-hexamethyl-2-(trimethylsilyl)trisilane (40).[38] A previously published procedure[38] was adapted as follows. A solution of HCCMgBr in THF (0.5 M, 23.74 mL, 11.868 mmol) was added dropwise to a stirred solution of $ClSi(TMS)_3$ (2.800 g, 9.890 mmol) in THF (20 mL) at 0 °C. The clear yellowish reaction mixture was stirred for 10 min at 0 °C and then for 18 h at room temperature. The reaction mixture was diluted with hexane (100 mL) and washed with saturated aq NH_4Cl (2 × 30 mL), and the clear slightly yellowish organic phase was dried over $MgSO_4$. Volatiles were removed under reduced pressure. Sublimation on a Kugelrohr distillation apparatus (90 °C, 800 mTorr) gave **40** as a white crystalline solid (2.424 g, 8.890 mmol, 90%).

Mp 100.3−101.5 °C. ^{1}H NMR (400 MHz, $CDCl_3$): δ 0.21 (s, 27H), 2.30 (s, 1H). ^{13}C NMR (100 MHz, $CDCl_3$): δ 0.2, 84.0, 95.8. IR (KBr): 3300, 3285, 2952, 2896, 2828, 2787, 2015, 1443, 1399, 1312, 1283, 1258, 1246, 835, 746, 691, 648, 622, 598, 472 cm^{-1}. MS m/z (%): 273.1 (32, M), 257.1 (100, M − CH_3). HRMS (CI) for ($C_{11}H_{28}Si_4^+$): calcd 272.1268, found 272.1273. Anal. Calcd for $C_{11}H_{28}Si_4$: C, 48.45; H, 10.35. Found: C, 48.48; H, 10.22, which is in agreement with the literature.[38]

Reaction of 39 with MeLi. To a colorless solution of **39** (230 mg, 0.517 mmol) in THF (20 mL) cooled to −78 °C was slowly added a solution of MeLi in ether (1.6 M, 356 μL, 0.569 mmol). The solution turned orange-brown immediately. The reaction mixture was stirred at this temperature for 60 min and then for an additional 60 min at 0 °C. The solution turned green-brown during this time. Progress of the reaction was monitored by TLC (hexane). The solution was diluted with ether (50 mL), washed with saturated aq NH_4Cl (1 × 30 mL), and the clear yellowish organic phase was dried over $MgSO_4$. Solvents were removed under reduced pressure, and the yellowish solid residue was purified using column chromatography on silica gel (hexane). Compounds were eluted from the column in the following order: **42** (130 mg, 0.496 mmol, 96%) and then **43** (95 mg, 0.480 mmol, 93%). Both compounds were obtained as colorless oils.

1,1,1,2,3,3,3-Heptamethyl-2-(trimethylsilyl)trisilane (42).[46,47] ^{1}H NMR (400 MHz, $CDCl_3$): δ 0.05 (s, 3H), 0.12 (s, 27H). ^{13}C NMR (100 MHz, $CDCl_3$): δ 0.4. IR (KBr): 2949, 2893, 2855, 2823, 1438, 1416, 1395, 1306, 1246, 835, 782, 744, 730, 687, 623 cm^{-1}. MS m/z (%): 262.1 (55, M), 247.1 (100, M − CH_3). HRMS (CI) for ($C_{10}H_{30}Si_4^+$): calcd 262.1425, found 262.1431. Anal. Calcd for $C_{10}H_{30}Si_4$: C, 45.72; H, 11.51. Found: C, 45.94; H, 11.70, which is in agreement with the literature.[46,47]

((4-Ethynylphenyl)ethynyl)trimethylsilane (43).[48] ^{1}H NMR (400 MHz, $CDCl_3$): δ 0.25 (s, 9H), 3.16 (s, 1H), 7.41 (s, 4H). ^{13}C NMR (100 MHz, $CDCl_3$): δ −0.1, 78.9, 83.2, 96.5, 104.3, 122.1, 123.6, 131.8, 131.9, which is in agreement with the literature.[48]

Synthesis of Silanes 44 and 45. A flame-dried Schlenk flask was charged with **24** (1.994 g, 5.000 mmol), $Pd(PPh_3)_4$ (83 mg, 0.072 mmol, 4 mol %), and CuI (10 mg, 0.054 mmol, 3 mol %). After three successive vacuum/argon cycles, dry and degassed THF (10 mL) and triethylamine (5 mL) were added from a syringe. Subsequently, TMSA (255 μL, 1.800 mmol) was added dropwise at room temperature. The yellow solution was stirred for 3 h at 40 °C. A dense white solid precipitated. The crude reaction mixture was diluted with ether (100 mL) and washed with saturated aq NH_4Cl (2 × 30 mL), and the

DOI: 10.1021/acs.joc.5b00661
J. Org. Chem. 2015, 80, 6173−6192

yellowish organic phase was dried over $MgSO_4$. Solvents were removed under reduced pressure, and the yellowish solid residue was purified using column chromatography on silica gel (hexane). Compounds were eluted from the column in the following order: **24** (1.258 g, 3.154 mmol) as a white crystalline solid, **44** (456 mg, 1.235 mmol, 69%) as a clear colorless oil, and **45** (153 mg, 0.451 mmol, 25%) as a white crystalline solid.

((2,3-Dichloro-4-iodophenyl)ethynyl)trimethylsilane (44). ^{1}H NMR (400 MHz, $CDCl_3$): δ 0.27 (s, 9H), 7.09 (d, J = 8.28 Hz, 1H), 7.70 (d, J = 8.28 Hz, 1H). ^{13}C NMR (100 MHz, $CDCl_3$): δ −0.3, 99.1, 100.3, 102.6, 125.0, 131.9, 134.4, 137.4, 137.6. IR (KBr): 2959, 2897, 2853, 2173, 2147, 1561, 1449, 1431, 1408, 1350, 1321, 1299, 1250, 1234, 1170, 1160, 1137, 1067, 900, 844, 815, 760, 686, 621, 581 cm^{-1}. MS m/z (%): 367.9 (12, M + H), 352.9 (14, M − CH_3), 73.0 (100, TMS). HRMS (CI) for ($C_{11}H_{11}Cl_2ISi$ + H^+): calcd 368.9130, found 368.9131. Anal. Calcd for $C_{11}H_{11}Cl_2ISi$: C, 35.79; H, 3.00. Found: C, 36.05; H, 3.26.

(2,3-Dichloro-1,4-phenylene)bis(ethyne-2,1-diyl)bis(trimethylsilane) (45). Mp 81.3−82.0 °C. ^{1}H NMR (400 MHz, $CDCl_3$): δ 0.27 (s, 18H), 7.32 (s, 2H). ^{13}C NMR (100 MHz, $CDCl_3$): δ −0.3, 100.7, 103.0, 124.7, 130.7, 135.1. IR (KBr): 2955, 2926, 2897, 2854, 2162, 1579, 1451, 1409, 1365, 1351, 1250, 1150, 948, 936, 866, 843, 829, 760, 698, 662, 630, 615, 600, 547 cm^{-1}. MS m/z (%): 339.1 (100, M + H), 323.0 (75, M − CH_3), 73.0 (65, TMS). HRMS (CI) for ($C_{16}H_{20}Cl_2Si_2$ + H^+): calcd 339.0559, found 339.0568. Anal. Calcd for $C_{16}H_{20}Cl_2Si_2$: C, 56.62; H, 5.94. Found: C, 56.69; H, 6.01.

2,3-Dichloro-1-ethynyl-4-iodobenzene (46). To a stirred solution of **44** (400 mg, 1.084 mmol) in wet THF (5 mL) was added a solution of TBAF in THF (1.0 M, 1.30 mL, 1.300 mmol) at room temperature. The yellowish reaction mixture was stirred for 30 min. The mixture was then diluted with ether (50 mL) and washed with water (1 × 20 mL), and the organic phase was dried over $MgSO_4$. Solvents were removed under reduced pressure, and column chromatography on silica gel (hexane) afforded **46** as a light and air sensitive white crystalline solid (290 mg, 0.977 mmol, 90%).

Mp 69.1−70.2 °C. ^{1}H NMR (400 MHz, $CDCl_3$): δ 3.46 (s, 1H), 7.12 (d, J = 8.27 Hz, 1H), 7.74 (d, J = 8.27 Hz, 1H). ^{13}C NMR (100 MHz, $CDCl_3$): δ 83.2, 84.2, 99.8, 124.0, 132.3, 134.5, 137.6, 137.7. IR (KBr): 3284, 2958, 2925, 2853, 2161, 2118, 1562, 1454, 1429, 1348, 1268, 1251, 1169, 1133, 1066, 864, 845, 814, 760, 683, 671, 630, 591, 576 cm^{-1}. MS m/z (%): 296.9 (100, M + H). HRMS (CI) for ($C_8H_3Cl_2I$ + H^+): calcd 296.8735, found 296.8744. Anal. Calcd for $C_8H_3Cl_2I$: C, 32.36; H, 1.02. Found: C, 32.73; H, 1.26.

2-((2,3-Dichlorophenyl)ethynyl)-1,1,1,3,3,3-hexamethyl-2-(trimethylsilyl)trisilane (47). A solution of LiHMDS in THF (1.0 M, 1.68 mL, 1.684 mmol) was added dropwise to a stirred solution of **46** (250 mg, 0.842 mmol) in THF (10 mL) at −78 °C. The clear purple solution was stirred for 60 min at −78 °C. Subsequently, $ClSi(TMS)_3$ (566 mg, 2.000 mmol) was added, and the solution was stirred for 30 min at −78 °C. Cooling was stopped, and the reaction mixture was slowly warmed to room temperature and stirred for an additional 18 h. The purple reaction mixture was diluted with ether (50 mL), washed with 5% aq HCl (1 × 25 mL), water (1 × 25 mL), and saturated aq NH_4Cl (2 × 25 mL), and the clear yellowish organic phase was dried over $MgSO_4$. Volatiles were removed under reduced pressure. Column chromatography on silica gel (hexane) gave **47** as a clear colorless liquid (266 mg, 0.637 mmol, 76%).

^{1}H NMR (400 MHz, $CDCl_3$): δ 0.26 (s, 27H), 7.10 (dd, J_1 = 7.67 Hz, J_2 = 8.14 Hz, 1H), 7.34 (dd, J_1 = 1.54 Hz, J_2 = 8.19 Hz, 1H), 7.35 (dd, J_1 = 1.54 Hz, J_2 = 7.61 Hz, 1H). ^{13}C NMR (100 MHz, $CDCl_3$): δ 0.4, 96.9, 104.0, 126.4, 126.7, 129.4, 131.5, 133.1, 134.4. IR (KBr): 3067, 2950, 2894, 1577, 1554, 1448, 1432, 1407, 1349, 1258, 1245, 1188, 1155, 1049, 895, 866, 836, 780, 746, 709, 691, 652, 623, 483 cm^{-1}. MS m/z (%): 417.1 (55, M + H), 384.1 (100). HRMS (APCI) for ($C_{17}H_{30}Cl_2Si_4$ + H^+): calcd 417.08744, found 417.08747. Anal. Calcd for $C_{17}H_{30}Cl_2Si_4$: C, 48.89; H, 7.24. Found: C, 48.97; H, 7.24.

■ ASSOCIATED CONTENT

Supporting Information

^{1}H and ^{13}C NMR spectra of all new compounds, solid state NMR spectra of 5%**1**@TPP-d_{12}(235) and 5%**2**@TPP-d_{12}(70), and an ORTEP view of a single molecule and packing in crystals of **16**, **17**, **20**, and **26**. The Supporting Information is available free of charge on the ACS Publications website at DOI: 10.1021/acs.joc.5b00661.

■ AUTHOR INFORMATION

Corresponding Author

*E-mail: kaleta@uochb.cas.cz.

Notes

The authors declare no competing financial interest.

■ ACKNOWLEDGMENTS

This work was supported by the European Research Council under the European Community Framework Programme (FP7/2007-2013), ERC Grant 227756, and by the Institute of Organic Chemistry and Biochemistry, Academy of Sciences of the Czech Republic (RVO 61388963). Y.S., K.Z., and C.T.R. gratefully acknowledge financial support from the US National Science Foundation Division of Materials Research through Grant DMR-1409981. We are grateful to Dr. Lucie Bednářová and Dr. Radek Pohl for help with IR and NMR spectra, respectively.

■ REFERENCES

(1) Schliwa, M., Ed. *Molecular Motors*; Wiley-VCH: Weinheim, Germany, 2003.
(2) Kottas, G. S.; Clarke, L. I.; Horinek, D.; Michl, J. *Chem. Rev.* **2005**, *105*, 1281−1376.
(3) Kinbara, K.; Aida, T. *Chem. Rev.* **2005**, *105*, 1377−1400.
(4) Khuong, T.-A. V.; Nuñez, J. E.; Godinez, C. E.; Garcia-Garibay, M. A. *Acc. Chem. Res.* **2006**, *39*, 413−422.
(5) Horansky, R. D.; Magnera, T. F.; Price, J. C.; Michl, J. *Lect. Notes Phys.* **2007**, *711*, 303−330.
(6) Crowley, J. D.; Kay, E. R.; Leigh, D. A. In *Intelligent Materials*; Shahinpoor, M., Schneider, H.-J., Eds.; Royal Society of Chemistry: Cambridge, UK, 2008; pp 1−47.
(7) Michl, J.; Sykes, E. C. H. *ACS Nano* **2009**, *3*, 1042−1048.
(8) Xue, M.; Wang, K. L. *Sensors* **2012**, *12*, 11612−11637.
(9) Lensen, D.; Elemans, J. A. A. W. *Soft Matter* **2012**, *8*, 9053−9063.
(10) Kobr, L.; Zhao, K.; Shen, Y.; Comotti, A.; Bracco, S.; Shoemaker, R. K.; Sozzani, P.; Clark, N. A.; Price, J. C.; Rogers, C. T.; Michl, J. *J. Am. Chem. Soc.* **2012**, *134*, 10122−10131.
(11) Kobr, L.; Zhao, K.; Shen, Y.; Shoemaker, R. K.; Rogers, C. T.; Michl, J. *Adv. Mater.* **2013**, *25*, 443−448.
(12) Lemouchi, C.; Iliopoulos, K.; Zorina, L.; Simonov, S.; Wzietek, P.; Cauchy, T.; Fortea, A.; Canadell, E.; Kaleta, J.; Michl, J.; Gindre, D.; Chrysos, M.; Batail, P. *J. Am. Chem. Soc.* **2013**, *135*, 9366−9376.
(13) Lemouchi, C.; Yamamoto, H. M.; Kato, R.; Simonov, S.; Zorina, L.; Rodriguez-Fortea, A.; Canadell, E.; Wzietek, P.; Illiopoulos, K.; Gindre, D.; Chrysos, M.; Batail, P. *Cryst. Growth Des.* **2014**, *14*, 3375−3383.
(14) Kobr, L.; Zhao, K.; Shen, Y.; Shoemaker, R. K.; Rogers, C. T.; Michl, J. *Cryst. Growth Des.* **2014**, *14*, 559−568.
(15) Zhao, K.; Dron, P. I.; Kaleta, J.; Rogers, C. T.; Michl, J. In *Topics in Current Chemistry - Molecular Machines and Motors: Recent Advances and Perspectives*; Credi, A., Silvi, S., Venturi, M., Eds.; Springer: Switzerland, 2014; Vol. 354, pp 163−211.
(16) Credi, A., Silvi, S., Venturi, M., Eds. *Molecular Machines and Motors*; Springer: Heidelberg, Germany, 2014.
(17) Kao, C.-Y.; Lu, H.-F.; Chao, I.; Yang, J.-S. *Org. Lett.* **2014**, *16*, 6100−6103.

DOI: 10.1021/acs.joc.5b00661
J. Org. Chem. 2015, 80, 6173−6192

(18) Inagaki, Y.; Yamaguchi, K.; Setaka, W. *RSC Adv.* **2014**, *4*, 58624−58630.
(19) Rozenbaum, V. M.; Ogenko, V. M.; Chuiko, A. A. *Phys.−Usp.* **1991**, *34*, 883−902.
(20) Allcock, H. R.; Siegel, L. A. *J. Am. Chem. Soc.* **1964**, *86*, 5140−5144.
(21) Kobr, L.; Zhao, K.; Shen, Y.; Polívková, K.; Shoemaker, R. K.; Clark, N. A.; Price, J. C.; Rogers, C. T.; Michl, J. *J. Org. Chem.* **2013**, *78*, 1768−1777.
(22) Cipolloni, M.; Kaleta, J.; Mašát, M.; Dron, P. I.; Shen, Y.; Zhao, K.; Rogers, C. T.; Shoemaker, R.; Michl, J. *J. Phys. Chem. C* **2015**, *119*, 8805−8820.
(23) Adcock, W.; Clark, C. I.; Trout, N. A. *J. Org. Chem.* **2001**, *66*, 3362−3371.
(24) Goldsmith, R.; Vura-Weis, J.; Scott, A.; Borkar, S.; Sen, A.; Ratner, M.; Wasielewski, M. *J. Am. Chem. Soc.* **2008**, *130*, 7659−7669.
(25) Nikitin, K.; Müller-Bunz, H.; Ortin, Y.; Muldoon, J.; McGlinchey, M. J. *J. Am. Chem. Soc.* **2010**, *132*, 17617−17622.
(26) Fowelin, C.; Schüpbach, B.; Terfort, A. *Eur. J. Org. Chem.* **2007**, *6*, 1013−1017.
(27) Onda, M.; Ueda, M.; Atsuki, M.; Yamaguchi, J.; Yamaguchi, I. *J. Mol. Struct.* **1986**, *147*, 77−84.
(28) Hurdis, E. C.; Smyth, C. P. *J. Am. Chem. Soc.* **1942**, *64*, 2212−2216.
(29) Murphy, S.; Yang, X.; Schuster, G. B. *J. Org. Chem.* **1995**, *60*, 2411−2422.
(30) Kaleta, J.; Mazal, C. *Org. Lett.* **2011**, *13*, 1326−1329.
(31) Kaleta, J.; Nečas, M.; Mazal, C. *Eur. J. Org. Chem.* **2012**, *25*, 4783−4796.
(32) Kobayashi, E.; Jiang, J.; Ohta, H.; Furukawa, J. *J. Polym. Sci., Part A: Polym. Chem.* **1990**, *28*, 2641−2650.
(33) Caskey, D. C.; Wang, B.; Zheng, X.; Michl, J. *Collect. Czech. Chem. Commun.* **2005**, *70*, 1970−1985.
(34) Von R. Schleyer, P.; Gleicher, G. J.; Cupas, C. A. *J. Org. Chem.* **1966**, *31*, 2014−2015.
(35) Shen, H.; Vollhardt, K. P. C. *Synlett* **2012**, *23*, 208−214.
(36) Chalifoux, W. A.; McDonald, R.; Ferguson, M. J.; Tykwinski, R. R. *Angew. Chem., Int. Ed.* **2009**, *48*, 7915−7919.
(37) Eisler, S.; Chahal, N.; McDonald, R.; Tykwinski, R. R. *Chem.—Eur. J.* **2003**, *9*, 2542−2550.
(38) Payne, M. M.; Parkin, S. R.; Anthony, J. E. *J. Am. Chem. Soc.* **2005**, *127*, 8028−8029.
(39) Zou, Ch.; Duhayon, C.; Maraval, V.; Chauvin, R. *Angew. Chem., Int. Ed.* **2007**, *46*, 4337−4341.
(40) Zhao, Y.; Slepkov, A. D.; Akoto, C. O.; McDonald, R.; Hegmann, F. A.; Tykwinski, R. R. *Chem.—Eur. J.* **2005**, *11*, 321−329.
(41) Comotti, A.; Simonutti, R.; Stramare, S.; Sozzani, P. *Nanotechnology* **1999**, *10*, 70−76.
(42) Comotti, A.; Bracco, S.; Ferretti, L.; Mauri, M.; Simonutti, R.; Sozzani, P. *Chem. Commun. (Cambridge, U.K.)* **2007**, 350−352.
(43) Ito, N.; Esaki, H.; Maesawa, T.; Imamiya, E.; Maegawa, T.; Sajiki, H. *Bull. Chem. Soc. Jpn.* **2008**, *81*, 278−286.
(44) Allcock, H. R.; Walsh, E. J. *Inorg. Chem.* **1971**, *10*, 1643−1647.
(45) Sheldrick, G. M. *Acta Crystallogr.* **2008**, *A64*, 112−122.
(46) Gilman, H.; Holmes, J. M.; Smith, C. L. *Chem. Ind. (Chichester, U.K.)* **1965**, 848−849.
(47) Ishikawa, M.; Iyoda, J.; Ikeda, H.; Kotake, K.; Hashimoto, T.; Kumada, M. *J. Am. Chem. Soc.* **1981**, *103*, 4845−4850.
(48) Liu, Y.; Jiang, S.; Glusac, K.; Powell, D. H.; Anderson, D. F.; Schanze, K. S. *J. Am. Chem. Soc.* **2002**, *124*, 12412−12413.

DOI: 10.1021/acs.joc.5b00661
J. Org. Chem. 2015, 80, 6173−6192